remains unknown; however, the cell type difference may be a likely reason. In support of this notion, even intact ApoE3 induces a very low level of lipid efflux from macrophages or fibroblasts, and ABCA1 transfection induces a marked lipid efflux mediated by intact ApoE3 in these cells (Smith et al., 1996; Remaley et al., 2001). In contrast, intact ApoE3 itself induces marked lipid efflux from astrocytes without ABCA1 transfection as shown in this study. This may be because apolipoprotein-mediated cholesterol efflux is only apparent in growth-arrested cells (Mendez, 1997).

We have observed that pretreatment with 22-hydroxylcholesterol enhanced ABCA1 expression in neurons and cholesterol efflux induced by ApoE, suggesting that ABCA1 is involved in ApoE- and 22-kDa-ApoE3-mediated cholesterol efflux (Fig. 6). The involvement of ABCA1 has been also demonstrated by the fact that the knockdown of ABCA1 significantly reduced lipid efflux induced by 22-kDa ApoEs (Fig. 7). One cannot exclude the possibility that factors other than ABCA1 that are relevant to biological mechanisms are involved because the involvement of ATP-binding cassette protein G1 has been reported previously (Karten et al., 2006; Kim et al., 2007); however, the lines of evidence in our present study suggest that lipid efflux from cultured neurons induced by ApoE or an ApoE fragment is mediated by ABCA1 function.

It is reasonable to assume that the disruption of the ApoE4 domain interaction by, for example, small molecules that create the ApoE3-like structure is a potential therapeutic target in neurodegenerative diseases including AD (Mahley et al., 2006). However, if the role of ApoE in HDL generation and its supply to neurons are critically involved in neurodegeneration in AD, other approaches that do not modulate the acceptor function, but modulate the cellular factors including ABCA1 expression and subsequent HDL generation, could also be candidate therapeutic targets.

REFERENCES

Bielicki JK, Johnson WJ, Weinberg RB, Glick JM, Rothblat GH. 1992. Efflux of lipid from fibroblasts to apolipoproteins: dependence on elevated levels of cellular unesterified cholesterol. J Lipid Res 33:1699–1709.

Borghini I, Barja F, Pometta D, James RW. 1995. Characterization of subpopulations of lipoprotein particles isolated from human cerebrospinal fluid. Biochim Biophys Acta 1255:192–200.

Boyles JK, Pitas RE, Wilson E, Mahley RW, Taylor JM. 1985. Apolipoprotein E associated with astrocytic glia of the central nervous system and with nonmyelinating glia of the peripheral nervous system. J Clin Invest 76:1501–1513.

Brooks-Wilson A, Marcil M, Clee SM, Zhang LH, Roomp K, van Dam M, Yu L, Brewer C, Collins JA, Molhuizen HO, Loubser O, Ouelette BF, Fichter K, Ashbourne-Excoffon KJ, Sensen CW, Scherer S, Mott S, Denis M, Martindale D, Frohlich J, Morgan K, Koop B, Pimstone S, Kastelein JJ, Hayden MR. 1999. Mutations in ABC1 in Tangier disease and familial high-density lipoprotein deficiency. Nat Genet 22: 336–345.

Corder EH, Saunders AM, Strittmatter WJ, Schmechel DE, Gaskell PC, Small GW, Roses AD, Haines JL, Pericak-Vance MA. 1993. Gene dose of apolipoprotein E type 4 allele and the risk of Alzheimer's disease in late onset families [see comments]. Science 261:921–923.

Demeester N, Castro G, Desrumaux C, De Geitere C, Fruchart JC, Santens P, Mulleners E, Engelborghs S, De Deyn PP, Vandekerckhove J, Rosseneu M, Labeur C. 2000. Characterization and functional studies of lipoproteins, lipid transfer proteins, and lecithin:cholesterol acyltransferase in CSF of normal individuals and patients with Alzheimer's disease. J Lipid Res 41:963–974.

Dong LM, Weisgraber KH. 1996. Human apolipoprotein E4 domain interaction. Arginine 61 and glutamic acid 255 interact to direct the preference for very low density lipoproteins. J Biol Chem 271:19053–19057.

Franceschini G, Calabresi L, Tosi C, Gianfranceschi G, Sirtori CR, Nichols AV. 1990. Apolipoprotein AIMilano. Disulfide-linked dimers increase high density lipoprotein stability and hinder particle interconversion in carrier plasma. J Biol Chem 265:12224–12231.

Gong JS, Kobayashi M, Hayashi H, Zou K, Sawamura N, Fujita SC, Yanagisawa K, Michikawa M. 2002. Apolipoprotein E (ApoE) isoform-dependent lipid release from astrocytes prepared from human ApoE3 and ApoE4 knock-in mice. J Biol Chem 277:29919–29926.

Hara H, Komaba A, Yokoyama S. 1992. Alpha-helical requirements for free apolipoproteins to generate HDL and to induce cellular lipid efflux. Lipids 27:302–304.

Hatters DM, Budamagunta MS, Voss JC, Weisgraber KH. 2005. Modulation of apolipoprotein E structure by domain interaction: differences in lipid-bound and lipid-free forms. J Biol Chem 280:34288–34295.

Karten B, Campenot RB, Vance DE, Vance JE. 2006. Expression of ABCG1, but not ABCA1, correlates with cholesterol release by cerebellar astroglia. J Biol Chem 281:4049–4057.

Kim WS, Rahmanto AS, Kamili A, Rye KA, Guillemin GJ, Gelissen IC, Jessup W, Hill AF, Garner B. 2007. Role of ABCG1 and ABCA1 in regulation of neuronal cholesterol efflux to apolipoprotein E discs and suppression of amyloid-beta peptide generation. J Biol Chem 282:2851–2861.

Krimbou L, Denis M, Haidar B, Carrier M, Marcil M, Genest J Jr. 2004. Molecular interactions between apolipoprotein E and the ATP-binding cassette transporter A1 (ABCA1): impact on ApoE lipidation. J Lipid Res 46:1457–1465.

LaDu MJ, Gilligan SM, Lukens JR, Cabana VG, Reardon CA, Van Eldik LJ, Holtzman DM. 1998. Nascent astrocyte particles differ from lipoproteins in CSF. J Neurochem 70:2070–2081.

Lawn RM, Wade DP, Garvin MR, Wang X, Schwartz K, Porter JG, Seilhamer JJ, Vaughan AM, Oram JF. 1999. The Tangier disease gene product ABC1 controls the cellular apolipoprotein-mediated lipid removal pathway. J Clin Invest 104:R25–31.

Lu B, Morrow JA, Weisgraber KH. 2000. Conformational reorganization of the four-helix bundle of human apolipoprotein E in binding to phospholipid. J Biol Chem 275:20775–20781.

Mahley RW, Weisgraber KH, Huang Y. 2006. Apolipoprotein E4: a causative factor and therapeutic target in neuropathology, including Alzheimer's disease. Proc Natl Acad Sci U S A 103:5644–5651.

Mendez AJ. 1997. Cholesterol efflux mediated by apolipoproteins is an active cellular process distinct from efflux mediated by passive diffusion. J Lipid Res 38:1807–1821.

Mendez AJ, Anantharamaiah GM, Segrest JP, Oram JF. 1994. Synthetic amphipathic helical peptides that mimic apolipoprotein A-I in clearing cellular cholesterol. J Clin Invest 94:1698–1705.

Michikawa M, Fan QW, Isobe I, Yanagisawa K. 2000. Apolipoprotein E exhibits isoform-specific promotion of lipid efflux from astrocytes and neurons in culture. J Neurochem 74:1008–1016.

Michikawa M, Gong JS, Fan QW, Sawamura N, Yanagisawa K. 2001. A novel action of Alzheimer's amyloid b-protein (Ab): oligomeric Ab promotes lipid release. J Neurosci 21:7226–7235.

Molander-Melin M, Blennow K, Bogdanovic N, Dellheden B, Mansson JE, Fredman P. 2005. Structural membrane alterations in Alzheimer brains found to be associated with regional disease development; increased density of gangliosides GM1 and GM2 and loss of cholesterol in detergent-resistant membrane domains. J Neurochem 92:171–182.

Morrow JA, Segall ML, Lund-Katz S, Phillips MC, Knapp M, Rupp B, Weisgraber KH. 2000. Differences in stability among the human apolipoprotein E isoforms determined by the amino-terminal domain. Biochemistry 39:11657–11666.

Morrow JA, Hatters DM, Lu B, Hochtl P, Oberg KA, Rupp B, Weisgraber KH. 2002. Apolipoprotein E4 forms a molten globule. A potential basis for its association with disease. J Biol Chem 277:50380–50385.

Nakai M, Kawamata T, Taniguchi T, Maeda K, Tanaka C. 1996. Expression of apolipoprotein E mRNA in rat microglia. Neurosci Lett 211:41–44.

Pitas RE, Boyles JK, Lee SH, Foss D, Mahley RW. 1987a. Astrocytes synthesize apolipoprotein E and metabolize apolipoprotein E–containing lipoproteins. Biochim Biophys Acta 917:148–161.

Pitas RE, Boyles JK, Lee SH, Hui D, Weisgraber KH. 1987b. Lipoproteins and their receptors in the central nervous system. Characterization of the lipoproteins in cerebrospinal fluid and identification of apolipoprotein B,E(LDL) receptors in the brain. J Biol Chem 262:14352–14360.

Raffai RL, Dong LM, Farese RV Jr, Weisgraber KH. 2001. Introduction of human apolipoprotein E4 "domain interaction" into mouse apolipoprotein E. Proc Natl Acad Sci U S A 98:11587–11591.

Ramaswamy G, Xu Q, Huang Y, Weisgraber KH. 2005. Effect of domain interaction on apolipoprotein E levels in mouse brain. J Neurosci 25:10658–10663.

Remaley AT, Stonik JA, Demosky SJ, Neufeld EB, Bocharov AV, Vishnyakova TG, Eggerman TL, Patterson AP, Duverger NJ, Santamarina-Fojo S, Brewer HB Jr. 2001. Apolipoprotein specificity for lipid efflux by the human ABCAI transporter. Biochem Biophys Res Commun 280:818–823.

Roheim PS, Carey M, Forte T, Vega GL. 1979. Apolipoproteins in human cerebrospinal fluid. Proc Natl Acad Sci U S A 76:4646–4649.

Saito H, Dhanasekaran P, Baldwin F, Weisgraber KH, Lund-Katz S, Phillips MC. 2001. Lipid binding-induced conformational change in human apolipoprotein E. Evidence for two lipid-bound states on spherical particles. J Biol Chem 276:40949–40954.

Saito H, Dhanasekaran P, Baldwin F, Weisgraber KH, Phillips MC, Lund-Katz S: 2003. Effects of polymorphism on the lipid interaction of human apolipoprotein E. J Biol Chem 278:40723–40729.

Saito H, Dhanasekaran P, Nguyen D, Deridder E, Holvoet P, Lund-Katz S, Phillips MC. 2004. Alpha-helix formation is required for high affinity binding of human apolipoprotein A-I to lipids. J Biol Chem 279:20974–20981.

Segall ML, Dhanasekaran P, Baldwin F, Anantharamaiah GM, Weisgraber KH, Phillips MC, Lund-Katz S. 2002. Influence of apoE domain structure and polymorphism on the kinetics of phospholipid vesicle solubilization. J Lipid Res 43:1688–1700.

Segrest JP, Jones MK, De Loof H, Brouillette CG, Venkatachalapathi YV, Anantharamaiah GM. 1992. The amphipathic helix in the exchangeable apolipoproteins: a review of secondary structure and function. J Lipid Res 33:141–166.

Smith JD, Miyata M, Ginsberg M, Grigaux C, Shmookler E, Plump AS. 1996. Cyclic AMP induces apolipoprotein E binding activity and promotes cholesterol efflux from a macrophage cell line to apolipoprotein acceptors. J Biol Chem 271:30647–30655.

Strittmatter WJ, Saunders AM, Schmechel D, Pericak-Vance M, Enghild J, Salvesen GS, Roses AD. 1993. Apolipoprotein E: high-avidity binding to beta-amyloid and increased frequency of type 4 allele in late-onset familial Alzheimer disease. Proc Natl Acad Sci U S A 90:1977–1981.

Vedhachalam C, Narayanaswami V, Neto N, Forte TM, Phillips MC, Lund-Katz S, Bielicki JK. 2007. The C-terminal lipid-binding domain of apolipoprotein E is a highly efficient mediator of ABCA1-dependent cholesterol efflux that promotes the assembly of high-density lipoproteins. Biochemistry 46:2583–2593.

Wang N, Silver DL, Thiele C, Tall AR. 2001. ATP-binding cassette transporter A1 (ABCA1) functions as a cholesterol efflux regulatory protein. J Biol Chem 276:23742–23747.

Weers PM, Narayanaswami V, Choy N, Luty R, Hicks L, Kay CM, Ryan RO. 2003. Lipid binding ability of human apolipoprotein E N-terminal domain isoforms: correlation with protein stability? Biophys Chem 100:481–492.

Weisgraber KH. 1990. Apolipoprotein E distribution among human plasma lipoproteins: role of the cysteine–arginine interchange at residue 112. J Lipid Res 31:1503–1511.

Weisgraber KH, Shinto LH. 1991. Identification of the disulfide-linked homodimer of apolipoprotein E3 in plasma. Impact on receptor binding activity. J Biol Chem 266:12029–12034.

Weisgraber KH, Roses AD, Strittmatter WJ. 1994. The role of apolipoprotein E in the nervous system. Curr Opin Lipidol 5:110–116.

Wetterau JR, Aggerbeck LP, Rall SC Jr, Weisgraber KH. 1988. Human apolipoprotein E3 in aqueous solution. I. Evidence for two structural domains. J Biol Chem 263:6240–6248.

Wilson C, Wardell MR, Weisgraber KH, Mahley RW, Agard DA. 1991. Three-dimensional structure of the LDL receptor-binding domain of human apolipoprotein E. Science 252:1817–1822.

Xu Q, Brecht WJ, Weisgraber KH, Mahley RW, Huang Y. 2004. Apolipoprotein E4 domain interaction occurs in living neuronal cells as determined by fluorescence resonance energy transfer. J Biol Chem 279:25511–15516.

Yancey PG, Bielicki JK, Johnson WJ, Lund-Katz S, Palgunachari MN, Anantharamaiah GM, Segrest JP, Phillips MC, Rothblat GH. 1995. Efflux of cellular cholesterol and phospholipid to lipid-free apolipoproteins and class A amphipathic peptides. Biochemistry 34:7955–7965.

Molecular Neurodegeneration

BioMed Central

Research article

Open Access

Apolipoprotein E4 (1–272) fragment is associated with mitochondrial proteins and affects mitochondrial function in neuronal cells

Toshiyuki Nakamura[1], Atsushi Watanabe[2], Takahiro Fujino[3], Takashi Hosono[1] and Makoto Michikawa*[1]

Address: [1]Department of Alzheimer's Disease Research, National Institute for Longevity Sciences, National Center for Geriatrics and Gerontology, 36-3 Gengo, Morioka, Obu, Aichi 474-8522, Japan, [2]Department of Vascular Dementia, National Institute for Longevity Sciences, National Center for Geriatrics and Gerontology, 36-3 Gengo, Morioka, Obu, Aichi 474-8522, Japan and [3]Department of Bioscience, Integrated Center for Science (INCS), Ehime University, Shizukawa, Shigenobu-cyo, Onsengun, Ehime 791-0295, Japan

Email: Toshiyuki Nakamura - nakamu-t@nifty.com; Atsushi Watanabe - watsushi@nils.go.jp; Takahiro Fujino - tfujino@m.ehime-u.ac.jp; Takashi Hosono - t-hos@nils.go.jp; Makoto Michikawa* - michi@nils.go.jp

* Corresponding author

Published: 20 August 2009

Molecular Neurodegeneration 2009, 4:35 doi:10.1186/1750-1326-4-35

Received: 8 July 2009
Accepted: 20 August 2009

This article is available from: http://www.molecularneurodegeneration.com/content/4/1/35

Abstract

Background: Apolipoprotein E allele ε4 (apoE4) is a strong risk factor for developing Alzheimer's disease (AD). Secreted apoE has a critical function in redistributing lipids among central nervous system cells to maintain normal lipid homeostasis. In addition, previous reports have shown that apoE4 is cleaved by a protease in neurons to generate apoE4(1–272) fragment, which is associated with neurofibrillary tanglelike structures and mitochondria, causing mitochondrial dysfunction. However, it still remains unclear how the apoE fragment associates with mitochondria and induces mitochondrial dysfunction.

Results: To clarify the molecular mechanism, we carried out experiments to identify intracellular apoE-binding molecules and their functions in modulating mitochondria function. Here, we found that apoE4 binds to ubiquinol cytochrome c reductase core protein 2 (UQCRC2) and cytochrome C1, both of which are components of mitochondrial respiratory complex III, and cytochrome c oxidase subunit 4 isoform 1 (COX IV 1), which is a component of complex IV, in Neuro-2a cells. Interestingly, these proteins associated with apoE4(1–272) more strongly than intact apoE4(1–299). Further analysis showed that in Neuro-2a cells expressing apoE4(1–272), the enzymatic activities of mitochondrial respiratory complexes III and IV were significantly lower than those in Neuro-2a cells expressing apoE4(1–299).

Conclusion: ApoE4(1–272) fragment expressed in Neuro2a cells is associated with mitochondrial proteins, UQCRC2 and cytochrome C1, which are component of respiratory complex III, and with COX IV 1, which is a member of complex IV. Overexpression of apoE4(1–272) fragment impairs activities of complex III and IV. These results suggest that the C-terminal-truncated fragment of apoE4 binds to mitochondrial complexes and affects their activities, and thereby leading to neurodegeneration.

Background

It has been shown that the prevalence of Alzheimer's disease (AD) is associated with the polymorphisms of genes related to cholesterol metabolism, including *apolipoprotein E (apoE)* [1-3], *ATP-binding cassette transporter A1 (ABCA1)* [4], and *CYP46*, the gene encoding cholesterol 24-hydroxylase [5,6]. Human apoE, a 34-kDa protein with 299 amino acids, has three major isoforms, apoE2, apoE3, and apoE4 [7-9]. It is well known that the possession of apoE4 allele is a major risk factor for Alzheimer's disease (AD) [1-3]. The apoE4 allele, which is found in 40–65% of cases of sporadic and familial AD, increases the occurrence and lowers the age of onset of the disease [3,10]. In the central nervous system, apoE is one of the major lipid acceptors [11,12] and interacts with ABCA1 [13] to remove cholesterol from cells and generate high-density lipoprotein (HDL) particles [14] in an apoE-isoform-specific manner [15-18]. Because apoE-HDL is the major cholesterol supplier in the brain and the supply of HDL-cholesterol is essential for synaptogenesis and neurite outgrowth in neurons [19,20], the apoE-isoform-dependent difference in HDL generation may result in the apoE-isoform-dependent difference in the maintenance of synaptic plasticity and the recovery of neurons from neuronal damage found in AD brains.

In addition to the role of apoE in modulating extracellular lipid transport, the isoform-dependent intracellular functions of apoE have also been reported. A previous report has shown that apoE3 recycling is associated with concomitant cholesterol efflux and thereby contributes to the formation of apoE-containing HDL, whereas apoE4 recycling is impaired and apoE4 accumulates within endosomal compartments, inducing an impaired cholesterol efflux [21], which may lead to the accumulation of cellular cholesterol and enhanced amyloid β-protein (Aβ) generation [22]. Another effect of reduced recycling of apoE4 is due to the tight binding of apoE4 to LDLR and LRP1 in the endosomal compartment [21], which in turn affects the interaction of the amyloid precursor protein (APP) and LRP1 that is crucial for the generation of Aβ [23,24]. Other lines of evidence have shown that apoE is cleaved by a protease to generate C-terminal-truncated fragments of apoE (residues 1–272) (apoE4(1–272)) in cultured neuronal cells, and the apoE(1–272) fragment is found in the brains of AD patients and transgenic mice expressing human apoE [25,26]. This proteolytic cleavage occurs in neurons, but not in astrocytes, and C-terminal-truncated fragments of apoE accumulated in an age-dependent manner in the brains of apoE4 mice and, to a significantly lesser extent, apoE3 mice [26]. These fragments, particularly apoE4(1–272), cause AD-like neurodegeneration and memory deficits in transgenic mice expressing apoE4(1–272) [27]. These lines of evidence suggest that the intraneuronal proteolytic processing of apoE could enhance the neuropathology and promote neurodegeneration in AD brains. It has been shown that the presence of a lipid-binding region of apoE (residues 244–272) is critical for apoE fragments to exert neurotoxicity in vivo [27]. Previous studies have shown that residues 267–299 are responsible for the tetramerization of apoE in solution, and the truncation of residues 273–299 in apoE4 gives rise to the monomeric form [28], and that these hydrophobic residues appear to be responsible for the neurotoxicity caused by the C-terminal-truncated apoE4 fragments [29]. In addition to the strong neurotoxicity caused by the apoE4(1–272) fragment, it has been shown that the apoE4(1–272) fragment accumulates in filamentous neurofibrillary tanglelike structures with phosphorylated tau in the cytosol or mitochondria, inducing mitochondrial dysfunction [25-27,29]. However, it still remains unclear how the apoE fragments are transported to the filamentous cytoplasmic structures or to mitochondria, and how they associate with mitochondria and induce mitochondrial dysfunction. To address these questions, we performed experiments to identify the proteins that associate with apoE4(1–272) or intact apoE4(1–299), and determine their functions. We identified three apoE4-binding proteins, all of which are components of mitochondria. We found that these proteins preferentially bind to apoE4(1–272) than to apoE4(1–299) and that the overexpression of apoE4(1–272) fragment decreases the enzymatic activities of mitochondrial respiratory complexes III and IV in cultured cells.

Results

Identification of apoE4-associated proteins

To identify molecules that specifically bind to apoE4, various fractions obtained from mouse brain were loaded onto a FLAG-apoE4(1–272) or FLAG-apoE4(1–299) affinity column. The proteins bound to these columns were eluted with an excess amount of FLAG peptide and the extracts were subjected to SDS-PAGE and silver staining. When each mouse brain fraction was loaded onto a FLAG-apoE4(1–272) or FLAG-apoE4(1–299) affinity column and eluted samples were subjected to SDS-PAGE, many protein bands were detected as candidate apoE4-associated proteins (Fig. 1). These bands were detected only when the mouse brain fractions and FLAG-apoE4 recombinant proteins coexisted.

To identify these proteins, the protein bands were subjected to LC-MS/MS analysis. As a result, we identified sixteen apoE4-associated proteins, which are shown in Table 1. These candidate proteins include the ATP synthase protein α and β subunits, which were previously reported [30]. Interestingly, ten among the candidate proteins are shown to be associated with mitochondria.

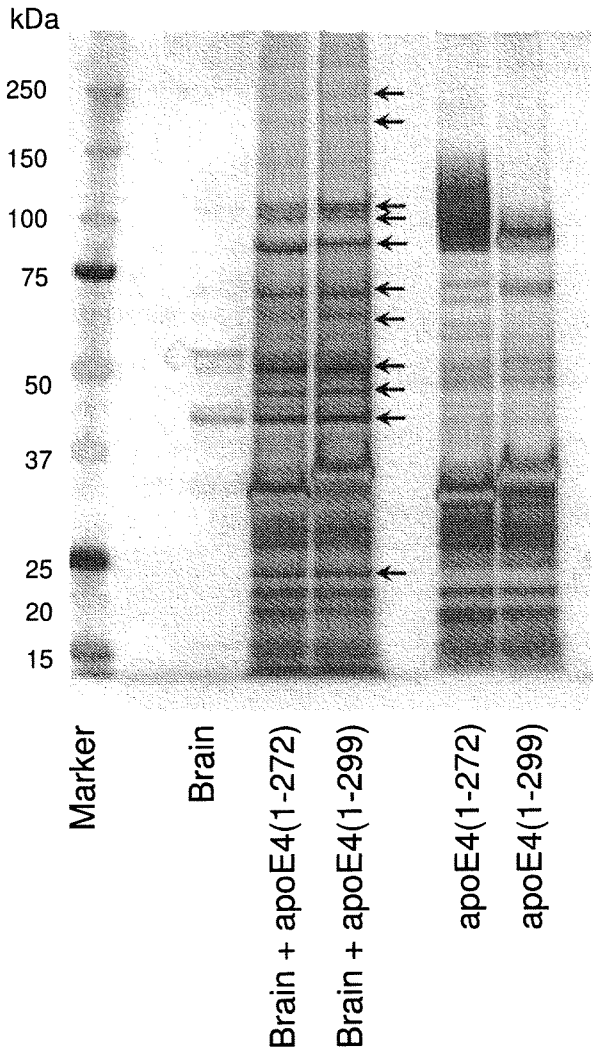

Figure 1
The proteins coimmunoprecipitated with apoE4 in the membrane extracts from mouse brain. Mouse brain membrane extracts were applied to the FLAG-apoE4(1–299) or FLAG-apoE4(1–272)-anti-FLAG M2-agarose affinity resin column and then eluted with the elution buffer. The eluant was dialyzed against the dialysis buffer, concentrated, and subjected to SDS-PAGE. The gels were stained with SilverQuest Silver Staining kit (Invitrogen). The protein bands (arrows), which were absent in the brain samples without apoE4s, and in the apoE4s samples without brain, were subjected to LC-MS/MS analysis.

Association of identified proteins with apoE4 in cultured cells

Next, we examined whether these proteins really associate with apoE in living cells. We cotransfected each candidate protein and FLAG-apoE4 into Neuro2a cells. Twenty-four hours following the transfection, the cells were harvested and treated with Triton X-100 solubilization buffer to obtain cell lysate as described in Materials and Methods. We carried out immunoprecipitation using these samples with an anti-FLAG antibody. The immunoprecipitate was then subjected to western blotting analysis using antibody specific for each protein or anti-HA antibody. This is because, in case we could not find antibodies specific for some candidate proteins, we could still generate HA-tagged proteins. Among the proteins identified by LC-MS/MS analysis, we found that three proteins, ubiquinol cytochrome c reductase core protein 2 (UQCRC2), cytochrome C1, and cytochrome *c* oxidase subunit 4 isoform 1 (COX IV 1) were associated with apoE4(1–299) and apoE4(1–272).

To examine whether mouse UQCRC2 is really associated with apoE proteins in cells, Neuro2a cells were cotransfected with mammalian expression plasmids encoding FLAG-apoE4(1–272) or FLAG-apoE4(1–299) and plasmids encoding mouse UQCRC2. Western blot analysis showed that the signal representing mouse UQCRC2 was clearly detected in the immunoprecipitate from the cells cotransfected with apoE4(1–272), while a very faint signal for UQCRC2 was detected in that from the cells cotransfected with apoE4(1–299). ApoE proteins were similarly immunoprecipitated in both samples (Fig. 2A). These results suggest that UQCRC2 prefers to associate with apoE4(1–272) than with apoE4(1–299).

To examine whether human UQCRC2 also associates with apoE4, we performed an experiment using human HA-tagged UQCRC2 expression vector. Similar to the results using mouse UQCRC2-transfected cells, the signals representing human HA-tagged UQCRC2 were clearly detected in the immunoprecipitate from the cells cotransfected with apoE4(1–272), while a very faint signal for HA-UQCRC2 was detected in that from the cells cotransfected with apoE4(1–299). Under these conditions, apoE4(1–272) and apoE4(1–299) proteins were similarly immunoprecipitated in both samples (Fig. 2B).

Next, we examined the association of human cytochrome C1 and apoE proteins using Neuro2a cells cotransfected with HA-tagged human cytochrome C1 expression vector and plasmids encoding FLAG-apoE4(1–272) or FLAG-apoE4(1–299). A strong signal for HA-tagged human cytochrome C1 was detected in the immunoprecipitate from the cell samples expressing apoE4(1–272), while a very faint signal for cytochrome C1 was detected in those transfected with apoE4(1–299) plasmid. ApoE4(1–272) and apoE4(1–299) proteins were similarly detected in both samples (Fig. 2C).

In addition, whether COX IV 1 is associated with apoE was determined. Human COX IV 1 was immunoprecipitated in the samples from apoE4(1–272)-expressing cells

Table 1: ApoE-associated proteins identified by LC-MS/MS analysis

Protein	Intracellular localization	Function
Solute carrier family 25 (mitochondrial carrier, Aralar) member 12	Mitochondria	Calcium-dependent mitochondrial aspartate and glutamate carrier
Ubiquinol cytochrome c reductase core protein 1	Mitochondria	Mitochondrial electron transport
* Ubiquinol cytochrome c reductase core protein 2 (UQCRC2)	Mitochondria	Mitochondrial electron transport
* Cytochrome C1	Mitochondria	Mitochondrial electron transport
Cytochrome oxidase subunit II	Mitochondria	Mitochondrial electron transport
* Cytochrome c oxidase subunit IV isoform 1 (COX IV1)	Mitochondria	Mitochondrial electron transport
ATP synthase, H+ transporting, mitochondrial F1 complex, α subunit, isoform 1	Mitochondria	ATP synthesis
ATP synthase, H+ transporting, mitochondrial F1 complex, β subunit	Mitochondria	ATP synthesis
ATP synthase, H+ transporting, mitochondrial F1 complex, δ subunit	Mitochondria	ATP synthesis
Methylenetetrahydrofolate dehydrogenase (NADP+ dependent)- 1 like	Mitochondria	Folic acid and derivative biosynthetic process
Syntaxin binding protein 1	Cytoplasm	Modulates exocytosis of dense-core granules
Nonmuscle myosin heavy chain	Cytoplasm	Actin filament-based movement
Tubulin, alpha 1A	Cytoplasm	Constituent of microtubules
RAB3A, member RAS oncogene family	Cytoplasm	Involved in exocytosis by regulating a late step in synaptic vesicle fusion.
Progesterone receptor membrane component 1	Plasma membrane	Receptor for progesterone
Cardiotrophin-like cytokine factor 1	Extracellular space	Cell surface receptor linked signal transduction

ApoE4-associated protein bands that were detected with SDS-PAGE were prepared and analyzed as described in the Methods. Asterisks (*) show the apoE-binding proteins identified and characterized in this study.

and a very faint signal for COX IV 1 was detected in the samples from apoE4(1–299)-expressing cells, whereas apoE4(1–272) and apoE4(1–299) proteins were similarly immunoprecipitated in both samples (Fig. 3). Interestingly, these proteins, UQCRC2, cytochrome C1, and COX IV 1, are associated more strongly with apoE4(1–272) than with apoE4(1–299). Concerning other proteins, we carried out similar experiments; however, no association of these proteins with apoE4(1–272) and apoE4(1–299) was found in cultured cells (data not shown).

The levels of apoE4 in mitochondrion-rich fraction isolated from ApoE4(1–272)- or ApoE4(1–299)-expressing cells

The results indicate that apoE4(1–272) binds to mitochondrial proteins; therefore, we next determined whether the levels of apoE4(1–272) and apoE4(1–299) are also associated with the mitochondria. We, thus, determined the levels of apoE4(1–272) and apoE4(1–299) in mitochondrion-rich fractions isolated from Neuro2a cells transfected with apoE4(1–272) or apoE4(1–299). The level of apoE4(1–272) in the pellet, a mitochondrion-rich fraction, was greater than that of apoE4(1–299) (Fig. 4). VDAC, a mitochondrion marker, was recovered in the pellet fraction (Fig. 4).

Effect of apoE4(1–272) overexpression on activities of mitochondrial respiratory complexes

It is known that UQCRC2 and cytochrome C1 are subunits of mitochondrial respiratory complex III and COX IV 1 is a subunit of mitochondrial respiratory complex IV. It

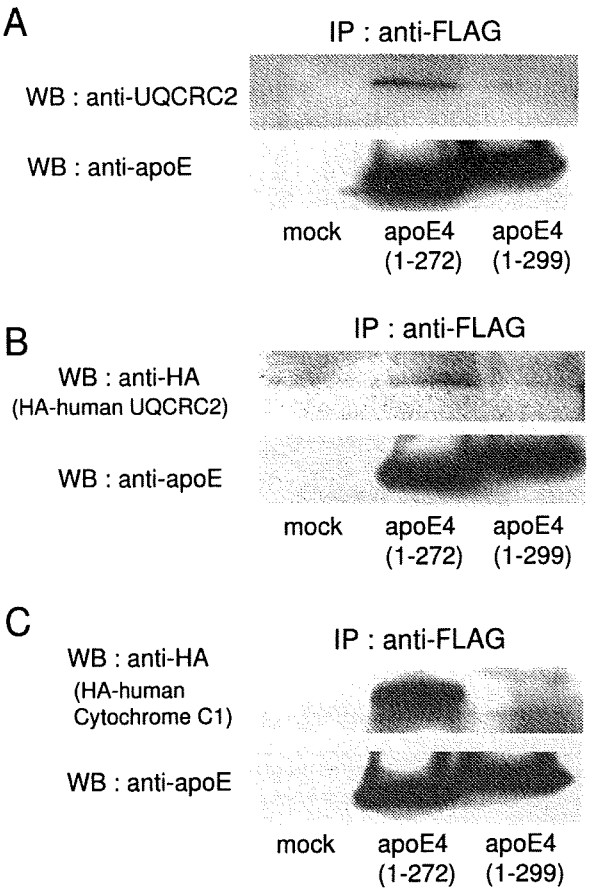

Figure 2
ApoE4 interacts with the subunits of mitochondrial respiratory complex III in Neuro2a cells. Neuro2a cells were cotransfected with mammalian expression plasmids encoding FLAG-apoE4(1–272) or FLAG-apoE4(1–299) and plasmids encoding mouse UQCRC2, human HA-UQCRC2, or human HA-cytochrome C1, all of which are candidate proteins suggested to be associated with apoE4 (Table 1). Twenty-four hours following the transfection, the cells were harvested and treated with 500 μl of Triton X-100 solubilization buffer to obtain cell lysate. The cell lysate was then incubated with anti-FLAG M2-agarose affinity resin, and the protein binding to the affinity column was eluted using FLAG peptide, and the eluted protein was then analyzed by western blotting with anti-UQCRC2 (mouse UQCRC2) antibody (A), anti-HA antibody (human UQCRC2) (B), or anti-HA antibody (human cytochrome C1) (C).

was reported that apoE4(1–272) induces mitochondrial dysfunction [25-27,29]. Because these proteins are associated more strongly with apoE4(1–272) than with apoE4(1–299), we investigated whether the enzymatic activities of mitochondrial respiratory complexes III and IV change, when apoE4(1–272) is overexpressed in cultured cells. Complex III activity was expressed as the difference in the reduction of cytochrome *c* with or without antimycin A and myxothiazol, both of which are complex III inhibitors. Expectedly, the complex III activity of apoE4(1–272)-overexpressing Neuro2a cells was lower than that of apoE4(1–299)-overexpressing cells (Fig. 5A). Because apoE4(1–272) associates with UQCRC2 and cytochrome C1, there was a possibility that the decrease in complex III activity in Neuro2a cells expressing apoE4(1–272) was due to the interaction between apoE4 and complex III. Complex IV activity was expressed as the difference in the oxidation of ferrocytochrome C with or without KCN and Na_3N, both of which are complex IV inhibitors. The complex IV activity of apoE4(1–272)-overexpressing cells was significantly lower than that of apoE4(1–299)-overexpressing cells (Fig. 5B). The levels of the mitochondrial proteins UQCRC2 and cytochrome C1 in apoE4(1–272)- and apoE4(1–299)-overexpressing cells were similar, as demonstrated by western blot analysis using anti-UQCRC2 and anti-cytochrome C1 antibodies (Fig. 5C).

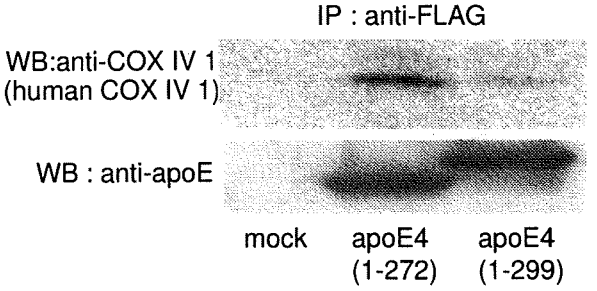

Figure 3
ApoE4 interacts with the subunits of mitochondrial respiratory complex IV in Neuro2a cells. Neuro2a cells were co-transfected with FLAG-apoE4 (1–272 or 1–299) plasmids and mammalian expression plasmids encoding the candidate apoE4-associated proteins. The cells were treated with 500 μl of Triton X-100 solubilization buffer and the cell lysate was incubated with anti-FLAG M2-agarose affinity resin. The immunoprecipitates were then analyzed by western blotting with an anti-COX IV 1 antibody (human COX IV 1).

Effects of overexpression of apoE4(1–272) and apoE4(1–299) on ATP synthase activity and mitochondrial membrane potential

Because apoE4(1–272) decreases the activities of mitochondrial complexes III and IV, we next examined whether the overexpression of apoE4(1–272) also affects ATP synthase activity and mitochondrial membrane potential. Unexpectedly, apoE4(1–272) and apoE4(1–299) showed no effect on ATP synthase activity (Fig. 6A). We further examined the effect of the overexpression of

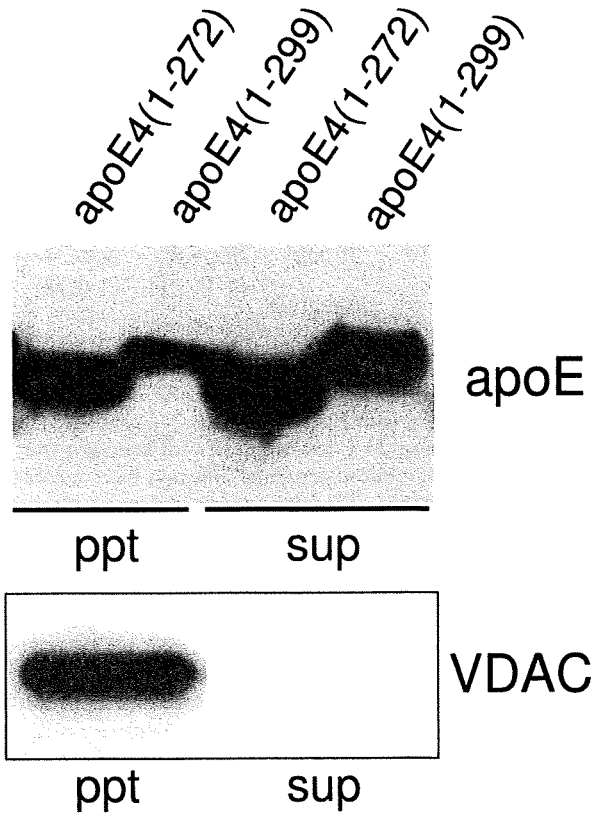

Figure 4
The level of apoE4(1–272) recovered from the mitochondrion-rich fraction is greater than that of apoE4(1–299). Neuro2a cells transfected with ApoE4(1–272) and ApoE4(1–299) plasmids were harvested and homogenized with a homogenizing buffer (10 mM Tris-HCl, pH 7.4, 1 mM EDTA, 0.25 M sucrose), and the resulting homogenate was centrifuged at 1,000 *g* for 10 min at 4°C. The resulting supernatant was further centrifuged at 8,000 *g* for 20 min at 4°C. The resulting precipitate (ppt) was used as the mitochondrion-rich fraction. Equal amounts of proteins from the ppt and supernatant (sup) fractions were analyzed by western blot analysis using the anti-apoE antibody, AB946, and the anti-VDAC antibody. VDAC was used as the mitochondrion marker.

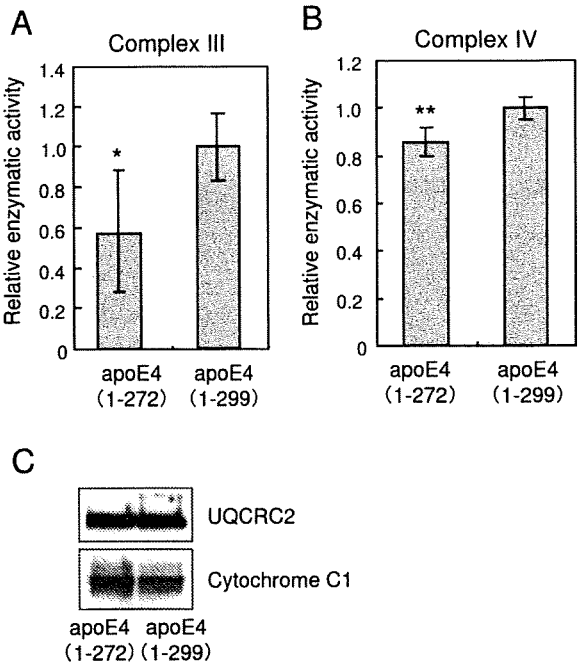

Figure 5
Overexpression of apoE4(1–272) results in the decreased level of complex III and IV activities. Enzymatic assays of respiratory chain complexes III (A) and IV (B) from Neuro2a cells overexpressing FLAG-apoE4(1–272 or 1–299) were determined as described in the Methods. The mitochondria levels in apoE4(1–272)- and apoE4(1–299)-overexpressing cells were determined by western blot analysis using the anti-UQCRC2 and the anti-cytochrome C1 antibodies (C). Data are the mean ± SEM of nine independent experiments. * $P < 0.005$, ** $P < 0.0005$ (t-distribution test).

apoE4(1–272) and apoE4(1–299) on mitochondrial membrane potential. Neuro2a cells transfected with these apoE4 species were stained with JC-1, a fluorescent dye that has been shown to be a reliable indicator of mitochondrial membrane potential changes in intact cells. After three hours of treatment of Neuro2a cells with 1 μM valinomycin, a K^+ ionophore that disrupts the transmembrane electrical gradient, the intensity of red fluorescence (FL2) markedly decreased, whereas that of green fluorescence (FL1) slightly increased, as demonstrated by JC-1 staining (Fig. 6B), indicating the dissipation of mitochondrial membrane potential. On the other hand, there were no significant differences in FL1 and FL2 intensities among Neuro2a cells transfected with mock, apoE4(1–272) and apoE4(1–299) (Figs. 6B, C, and 6D), indicating that the overexpression of apoE4(1–272) and apoE4(1–299) has no effect on mitochondrial membrane potential.

Discussion

Here, we show the molecules associated with apoE protein. Among the molecules identified, we show for the first time that apoE4, particularly C-terminal cleaved apoE4(1–272), binds to UQCRC2 cytochrome C1 and COX IV 1. Although apoE(1–272) has been shown to be translocated to mitochondria, it still remains unclear how the apoE fragments associate with mitochondria and induce mitochondrial dysfunction. The present study has shown that apoE4(1–272) binds to UQCRC2 cytochrome C1, a component of complex III, and COX IV 1, a component of complex IV, and that overexpression of apoE(1–

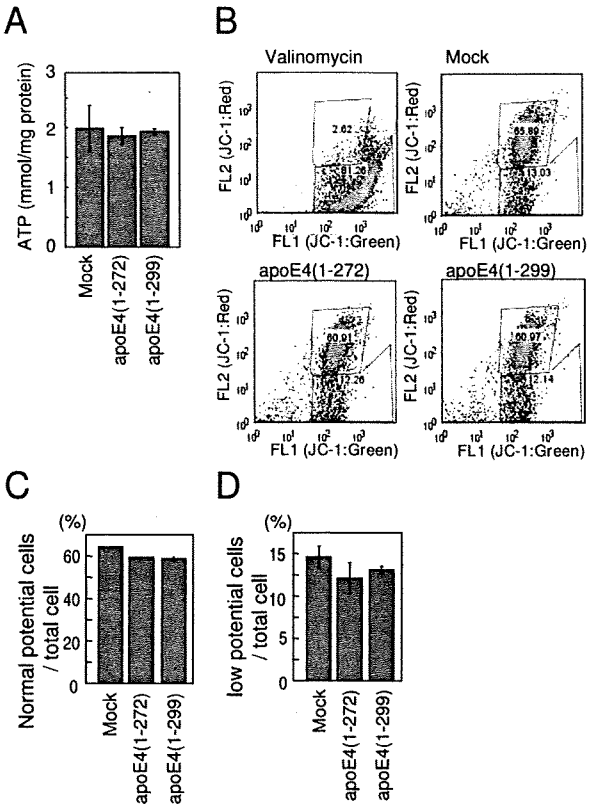

Figure 6
Effects of overexpression of apoE4(1–272) and apoE4(1–299) on ATP synthase activity and mitochondrial membrane potential. The ATP synthase activity in Neuro2a cells transfected with the ApoE4(1–272) and ApoE4(1–299) plasmids were determined (A) as described in the Methods. The data are the mean ± SEM of three experiments. (B) Flow cytometry plots were used to determine the ratio of cells having normal and low mitochondrial membrane potentials, which were demonstrated by staining with the JC-1 dye. The distribution of the cells sorted by FACS was analyzed, and the ratios of the number of cells showing normal membrane potential (C) and low membrane potential (D) to total cell number were calculated.

272) fragment in Neuro2a cells results in decreases in the levels of complex III and complex IV activities compared with those in cells overexpressing intact apoE4. These results suggest that the apoE4(1–272) fragment binds to UQCRC2 cytochrome C1 and COX IV 1, thereby inhibiting complex III and complex IV activities, respectively. The candidate molecules, which may associate with apoE to transport apoE to mitochondria, were not identified in our present analysis (Table 1). This should be addressed in a future study.

Another finding in the present study is that UQCRC2 cytochrome C1 and COX IV 1 are associated more strongly with ApoE4(1–272) than with intact apoE4(1–299) (Figs. 2, 3). There are at least two possible explanations for this result. One explanation is that apoE4(1–272) is structurally different from apoE4(1–299), resulting in the difference in hydrophobicity or binding affinity to other proteins. It has been shown that the C-terminus of apoE (residues 253–289) participates in hydrophobic interactions that stabilize the tetramer [28], and that these hydrophobic residues are suggested to be responsible for inducing neurotoxicity caused by the C-terminal-truncated apoE4 [29]. In addition, a recent study has shown that apoE4 lacking a hydrophobic C-terminal α-helical segment (residues 273–299) found in brain leads to a less organized C-terminal structure that is available for interaction with cell membranes and other proteins such as Aβ [31]. Another explanation is that more apoE(1–272) is translocated to mitochondria than intact apoE(1–299), because the silver staining shows that the intensities of the bands representing apoE-associated proteins were not different between the samples containing apoE4(1–272) and apoE4(1–299) (Fig. 1), whereas the level of apoE4(1–272) was greater than that of apoE4(1–299) in the mitochondrion-rich fraction of Neuro2a cells expressing apoE4(1–272) and apoE4(1–299) (Fig. 4). Although the precise mechanism underlying this difference is yet unknown, it is possible that the truncation of residues 273–299 in apoE4 leads to the reorganization of the C-terminal domain, with a lipid-binding region being less organized and available for hydrophobic interaction including Aβ [31-33].

Regarding the mitochondrial dysfunction in Alzheimer disease, there are previous reports showing that the overexpression of amyloid precursor protein increases the level of Aβ in mitochondria [34], and that mitochondrial complex III and IV activities are decreased in Tg2576 mouse brains [34]. In addition, the complex IV activity was shown to decrease in the brain of AD patients [35-39]. Moreover, it has been shown that the apoE(1–272) fragment is generated at a greater level from apoE4 than apoE3, and the overexpression of apoE isoform-dependently affects mitochondrial function [27]. These lines of evidence together with our present study suggest that the greater level of apoE4(1–272) fragment generated from apoE4 may be associated with Aβ that is transported to mitochondria and binds to UQCRC2 cytochrome C1 and COX IV 1, and causes mitochondrial dysfunction.

Complexes III and IV are related to ATP synthesis and the maintenance of mitochondrial membrane potential, which are critical for cell survival. Thus, we examined the

effect of the transient expressions of apoE4(1–272) and apoE4(1–299) on ATP synthesis and membrane potential in Neuro2a cells. Unexpectedly, there was no difference between apoE4(1–272)- and apoE4(1–299)-transfected cells in terms of the levels of ATP synthesis or membrane potential (Fig. 6). However, when we tried to generate the Neuro2a cells, in which apoE4(1–272) is stably expressed, all the cells were dead within 2 weeks after the transfection, whereas apoE4(1–299)-expressing cells remained alive. These results suggest that apoE4(1–272) may have neurotoxicity as previously reported [29], although the level of toxicity is low. This issue remains to be addressed in further studies.

One may consider that apoE is synthesized as a secretory protein; however, how apoE enters the cytosol remains unclear and controversial. Previous studies have shown that apoE escapes the secretory or endosomal internalization pathway, and enters the cytosol of neuronal cells [25,29,40] and non-neuronal cells [41], whereas another study has failed to show this [42]. Therefore, the physiological relevance of the three mitochondrial proteins that we have identified in this study, which are associated with apoE, remains to be confirmed under physiological conditions.

It is well known that apoE4 is a strong risk factor for AD development, and the regulation of apoE4 function may be a therapeutic target for AD. Our findings indicate that if we could modulate the generation of apoE4(1–272) and/or modulate its translocation to mitochondria, the apoE4-associated induction of neurodegeneration could be prevented or attenuated. Because it has been shown that the C-terminus of the apoE-cleaving enzyme is a neuron-specific, chymotrypsin-like serine protease [25-27], the characterization and modulation of this enzyme activity would be a therapeutic target for AD.

Conclusion

We identified intracellular apoE-binding molecules and determined their functions in modulating mitochondria function. The ApoE-binding molecules we found are ubiquinol cytochrome *c* reductase core protein 2 (UQCRC2), cytochrome C1, and cytochrome *c* oxidase subunit 4 isoform 1 (COX IV 1). The UQCRC2 and cytochrome C1 are components of mitochondrial respiratory complex III, and COX IV 1 is a component of complex IV. Interestingly, these proteins associated with apoE4(1–272) more strongly than intact apoE4 (1–299). When apoE4(1–272) expression level increased in Neuro2a cells, the enzymatic activities of mitochondrial respiratory complexes III and IV were significantly lower than those in Neuro-2a cells expressing apoE4(1–299). These results suggest that the C-terminal-truncated fragment of apoE4(1–272) bind to mitochondrial complexes and affects their activities.

Methods

Preparation of mouse brain membrane extracts and cytosolic fraction

Brains obtained from C57BL6 male mice were homogenized with a homogenizing buffer (10 mM Tris-HCl, pH 7.4 1 mM EDTA 0.25 M sucrose), and the homogenate was centrifuged at 1,000 *g* for 10 min at 4°C. The supernatant was recentrifuged at 10,000 *g* for 20 min at 4°C, and the resulting precipitate was suspended in a homogenizing buffer. The supernatant was recentrifuged at 100,000 *g* for 1 min at 4°C, and the resulting precipitate was suspended in a homogenizing buffer. The supernatant was used as the cytosolic fraction. The proteins in the 10,000 *g* and 100,000 *g* pellet fraction were extracted with homogenizing buffer containing 1 M KCl. The resulting pellet was solubilized with 2% Triton X-100 for 1 h at 4°C and then centrifuged at 100,000 *g* of 1 h at 4°C. The supernatants were used as 10,000 *g* or 100,000 *g* membrane extracts.

FLAG fusion proteins

Recombinant FLAG-apoE4 fusion proteins encoding WT (1–299) or C-terminal truncated apoE4 (1–272) were prepared and purified as follows. PCR products encoding apoE4 (1–272) and apoE4 (1–299) were subcloned into pFLAG-MAC expression vector (Sigma). These plasmids were transformed into the BL21 strain of *Escherichia coli* and induced with isopropyl-1-thio-b-$_D$-galactopyranoside to produce FLAG fusion proteins. The bacteria were suspended in PBS, and vigorous sonication was performed before centrifugation at 10,000 *g* for 20 min. The resulting supernatants were applied to anti-FLAG M2-agarose affinity resin column (Sigma) and then eluted with an elution buffer (TBS containing 100 μg/ml FLAG peptide (Sigma)). Purified FLAG fusion proteins were dialyzed against TBS.

FLAG-ApoE4 affinity chromatography and LC-MS/MS analysis

Recombinant FLAG-apoE4(1–299) or FLAG-apoE4(1–272) fusion protein coupled to anti-FLAG M2-agarose affinity resin was used to identify affinity-purified apoE4-binding proteins. The fractionated mouse brain samples were applied to the FLAG-apoE4(1–299)- and FLAG-apoE4(1–272)-anti-FLAG M2-agarose affinity resin column. The proteins bound to the resin column were then eluted with the elution buffer. The eluted proteins were dialyzed against the dialysis buffer, concentrated, and subjected to SDS-PAGE. The gels were stained with SilverQuest Silver Staining kit (Invitrogen). The proteins specifically associated with apoEs demonstrated as silver-

stained bands were cut out, digested with trypsin, and subjected to LC-MS/MS analysis.

LC-MS/MS analysis

The proteins in the silver-stained bands were reduced with 10 mM dithiothreitol at room temperature for 2 h and alkylated with 40 mM iodoacetamide in the dark at room temperature for 30 min. Each sample was digested with trypsin (4 μg/ml; Trypsin Gold, Promega) in 40 mM NH_4HCO_3/10%ACN at 37°C overnight. The extracted peptides were then separated via nano liquid chromatography (LC) (Paradigm MS4, Michrom BioResources, Inc., Auburn, CA) using a Magic C18 column (0.2 × 50 mm; Michrom BioResources, Inc.; Auburn, CA). The LC eluent was analyzed using an LCQ Advantage MAX mass spectrometer (Thermo Fisher Scientific) equipped with an ion-spray source. All MS/MS spectra were searched by SEQUEST algorithm from BioWorks software (Thermo Fisher Scientific).

Cells

Neuro2a cells were grown in DMEM medium, supplemented with 10% FBS, 50 units/ml penicillin, 50 mg/ml streptomycin, and 2 mM glutamine at 37°C in a humidified 5% CO_2 95% air incubator.

Transfection of plasmids into cells and co-immunopricipitation

PCR products encoding apoE4 (1-272) and apoE4 (1-299) were subcloned into pFLAG-CMV-2 expression vector (Sigma). Neuro2a cells were co-transfected with FLAG-apoE4 (1-272 or 1-299) plasmids and mammalian expression plasmids coding the candidate of apoE4 associating proteins (Toyobo, Japan) using Lipofectamine 2000 (Invitrogen, CA, USA). As necessary, mammalian expression plasmids coding the candidate apoE4-associated proteins were fused with HA-tag of their C-terminus using KOD-PLUS Mutagenesis Kit (Toyobo). The plasmids were transfected to Neuro2a cells as follows. Neuro2a cells were plated on a 6-cm plate at a cell density of 1.5 × 10^6 and cultured in the culture medium described above. The next day, the ells were transfected with the plasmid employing Lipofectamine 2000 reagent. On culture day 3, the cells were lysed with 500 μl of Triton X-100 solubilization buffer (10 mM Tris-HCl (pH 7.4), 150 mM NaCl, 1 mM EDTA, 10 mg/ml leupeptin, 1 mM PMSF, 0.5% Triton X-100). The cell lysate was incubated with anti-FLAG M2-agarose affinity resin. After an overnight incubation at 4°C, the beads were washed three times with Triton X-100 solubilization buffer and then eluted with the elution buffer (PBS containing FLAG peptide at a concentration of 100 μg/ml). The immunoprecipitates were then analyzed by western blotting with anti-HA monoclonal antibody (Sigma), anti-UQCRC2 monoclonal antibody (Abcam), and anti-COX IV 1 monoclonal antibody (Cell Signaling).

Enzymatic analysis of complexes III and IV

Mitochondria isolated from homogenates of Neuro2a cells transfected with ApoE4 (1-299 or 1-272) were used for enzymatic analysis.

(a) Complex III (Ubiquinol cytochrome c reductase)

The oxidation of ubiquinol$_2$ by complex III was determined using cytochrome *c* (III) as an electron acceptor. The assay was carried out in an assay medium (25 mM potassium phosphate buffer (pH 8.0), 1 mM EDTA, 1 mM KCN, 3 mM Na_3N) supplemented with 20 μM cytochrome *c* (III), and 20 μM ubiquinol$_2$. The reaction was started with 5 μg of mitochondrial protein and the enzyme activity was measured at 550 nm. The activity of complex III is estimated to be the difference in the reduction of cytochrome *c* with and without 10 μg/ml antimycin A and 10 μg/ml myxothiazol.

(b) Complex IV (Cytochrome c Oxidase)

The enzyme activity of cytochrome *c* oxidase (complex IV) was determined using Mitochondria Activity Assay kit (BioChain Institute, U.S.A.) and performed following the manufacture's procedure. Complex IV activity was measured as the oxidation of ferrocytochrome *c* by cytochrome *c* oxidase at 550 nm. Complex IV activity is expressed as the difference in the oxidation of ferrocytochrome C with or without KCN and Na_3N as complex IV inhibitor.

ATP synthase activity assay

Neuro2a cells transfected with apoE4(1-272) and apoE4(1-299) plasmids were harvested and homogenized with a homogenizing buffer (10 mM Tris-HCl, pH 7.4, 1 mM EDTA, 0.25 M sucrose), and the homogenate was centrifuged at 1,000 *g* for 10 min at 4°C. The resulting supernatant was further centrifuged at 10,000 × g for 20 min at 4°C, and the resulting pellet (ppt) fractions were obtained. The ppt fractions were resuspended in 100 μl of assay buffer (1 mM ADP and 5 mM sodium succinate) and incubated for 5 min at 37°C. 100 mM Tris-HCl buffer (pH 7.6) containing 4 mM EDTA was added and the fractions were further incubated for 2 min at 100°C. Then the fractions were plated on ice and ATP level in each fraction was determined using an ATP bioluminescence assay kit CLS II (Roche Diagnosis GmbH, Mannheim, Germany).

Analysis of mitochondrial membrane potential (mt)

ApoE4(1-272 or 1-299)-transfected Neuro2a cells were stained with 2 μM JC-1 (Molecular Probes, Eugene, OR) at 37°C for 20 min. Then, the cells were analyzed using a flow cytometer FACSCalibur (Becton Dickinson, Franklin Lakes, NJ) with FlowJo software (Tree Star Inc., Ashland, OR).

Statistical analysis

StatView computer software (Windows) was used for statistical analysis. Statistical significance of differences

between samples was evaluated by multiple pairwise comparisons among the sets of data using ANOVA and the Bonferoni t-test.

Competing interests

The authors declare that they have no competing interests.

Authors' contributions

TN carried out major part of the experiments. AW carried out TOF-MS/MS analysis and identified molecules associated with apoE. TF generated plasmid containing intact apoE3 and apoE4 cDNA. TH prepared cultured cells. MM designed this study and was involved in the interpretation of the results and in drafting the manuscript.

Acknowledgements

This work was supported by Grant-in-Aid for Scientific Research on Priority Areas-Research on Pathomechanisms of Brain Disorders-from the Ministry of Education, Culture, Sports, Science and Technology of Japan, a grant from the Program for Promotion of Fundamental Studies in Health Sciences of the National Institute of Biomedical Innovation (NIBRO), and a rant from the Ministry of Health, Labor and Welfare of Japan (Comprehensive Research on Aging and Health Grant H20-007).

References

1. Strittmatter WJ, Saunders AM, Schmechel D, Pericak-Vance M, Enghild J, Salvesen GS, Roses AD: **Apolipoprotein E: high-avidity binding to beta-amyloid and increased frequency of type 4 allele in late-onset familial Alzheimer disease.** *Proc Natl Acad Sci USA* 1993, **90**:1977-1981.
2. Roses AD: **Apolipoprotein E affects the rate of Alzheimer disease expression: beta-amyloid burden is a secondary consequence dependent on APOE genotype and duration of disease.** *J Neuropathol Exp Neurol* 1994, **53**:429-37.
3. Corder EH, Saunders AM, Strittmatter WJ, Schmechel DE, Gaskell PC, Small GW, Roses AD, Haines JL, Pericak-Vance MA: **Gene dose of apolipoprotein E type 4 allele and the risk of Alzheimer's disease in late onset families.** *Science* 1993, **261**:921-923.
4. Wollmer MA, Streffer JR, Lutjohann D, Tsolaki M, Iakovidou V, Hegi T, Pasch T, Jung HH, Bergmann K, Nitsch RM, Hock C, Papassotiropoulos A: **ABCA1 modulates CSF cholesterol levels and influences the age at onset of Alzheimer's disease.** *Neurobiol Aging* 2003, **24**:421-426.
5. Kolsch H, Lutjohann D, Ludwig M, Schulte A, Ptok U, Jessen F, von Bergmann K, Rao ML, Maier W, Heun R: **Polymorphism in the cholesterol 24S-hydroxylase gene is associated with Alzheimer's disease.** *Mol Psychiatry* 2002, **7**:899-902.
6. Papassotiropoulos A, Streffer JR, Tsolaki M, Schmid S, Thal D, Nicosia F, Iakovidou V, Maddalena A, Lutjohann D, Ghebremedhin E, Hegi T, Pasch T, Traxler M, Bruhl A, Benussi L, Binetti G, Braak H, Nitsch RM, Hock C: **Increased brain beta-amyloid load, phosphorylated tau, and risk of Alzheimer disease associated with an intronic CYP46 polymorphism.** *Arch Neurol* 2003, **60**:29-35.
7. Mahley RW: **Apolipoprotein E: cholesterol transport protein with expanding role in cell biology.** *Science* 1988, **240**:622-630.
8. Mahley RW, Huang Y: **Apolipoprotein E: from atherosclerosis to Alzheimer's disease and beyond.** *Curr Opin Lipidol* 1999, **10**:207-17.
9. Mahley RW, Rall SC Jr: **Apolipoprotein E: far more than a lipid transport protein.** *Annu Rev Genomics Hum Genet* 2000, **1**:507-37.
10. Farrer LA, Cupples LA, Haines JL, Hyman B, Kukull WA, Mayeux R, Myers RH, Pericak-Vance MA, Risch N, van Duijn CM: **Effects of age, sex, and ethnicity on the association between apolipoprotein E genotype and Alzheimer disease. A meta-analysis. APOE and Alzheimer Disease Meta Analysis Consortium.** *JAMA* 1997, **278**:1349-1356.
11. Roheim PS, Carey M, Forte T, Vega GL: **Apolipoproteins in human cerebrospinal fluid.** *Proc Natl Acad Sci USA* 1979, **76**:4646-4649.
12. Pitas RE, Boyles JK, Lee SH, Hui D, Weisgraber KH: **Lipoproteins and their receptors in the central nervous system. Characterization of the lipoproteins in cerebrospinal fluid and identification of apolipoprotein B, E(LDL) receptors in the brain.** *J Biol Chem* 1987, **262**:14352-14360.
13. Krimbou L, Denis M, Haidar B, Carrier M, Marcil M, Genest J: **Molecular interactions between apolipoprotein E and the ATP-binding cassette transporter A1 (ABCA1): Impact on ApoE lipidation.** *J Lipid Res* 2004, **45**:839-848.
14. Ito J, Zhang LY, Asai M, Yokoyama S: **Differential generation of high-density lipoprotein by endogenous and exogenous apolipoproteins in cultured fetal rat astrocytes.** *J Neurochem* 1999, **72**:2362-2369.
15. Michikawa M, Fan QW, Isobe I, Yanagisawa K: **Apolipoprotein E exhibits isoform-specific promotion of lipid efflux from astrocytes and neurons in culture.** *J Neurochem* 2000, **74**:1008-1016.
16. Gong JS, Kobayashi M, Hayashi H, Zou K, Sawamura N, Fujita SC, Yanagisawa K, Michikawa M: **Apolipoprotein E (ApoE) isoform-dependent lipid release from astrocytes prepared from human ApoE3 and ApoE4 knock-in mice.** *J Biol Chem* 2002, **277**:29919-29926.
17. Xu Q, Brecht WJ, Weisgraber KH, Mahley RW, Huang Y: **Apolipoprotein E4 domain interaction occurs in living neuronal cells as determined by fluorescence resonance energy transfer.** *J Biol Chem* 2004, **24**:25511-25516.
18. Gong JS, Morita SY, Kobayashi M, Handa T, Fujita SC, Yanagisawa K, Michikawa M: **Novel action of apolipoprotein E (ApoE): ApoE isoform specifically inhibits lipid-particle-mediated cholesterol release from neurons.** *Mol Neurodegener* 2007, **2**:9.
19. Mauch DH, Nagler K, Schumacher S, Goritz C, Muller EC, Otto A, Pfrieger FW: **CNS synaptogenesis promoted by glia-derived cholesterol.** *Science* 2001, **294**:1354-7.
20. Hayashi H, Campenot RB, Vance DE, Vance JE: **Glial lipoproteins stimulate axon growth of central nervous system neurons in compartmented cultures.** *J Biol Chem* 2004, **279**:14009-15.
21. Heeren J, Grewal T, Laatsch A, Becker N, Rinninger F, Rye K-A, Beisiegel U: **Impaired Recycling of Apolipoprotein E4 Is Associated with Intracellular Cholesterol Accumulation.** *J Biol Chem* 2004, **279**:55483-55492.
22. Fassbender K, Simons M, Bergmann C, Stroick M, Lutjohann D, Keller P, Runz H, Kuhl S, Bertsch T, von Bergmann K, Hennerici M, Beyreuther K, Hartmann T: **Simvastatin strongly reduces levels of Alzheimer's disease beta-amyloid peptides Abeta 42 and Abeta 40 in vitro and in vivo.** *Proc Natl Acad Sci USA* 2001, **98**:5856-61.
23. Cole SL, Vassar R: **The Alzheimer's disease beta-secretase enzyme, BACE1.** *Mol Neurodegener* 2007, **2**:22.
24. Cam JA, Zerbinatti CV, Li Y, Bu G: **Rapid endocytosis of the low density lipoprotein receptor-related protein modulates cell surface distribution and processing of the beta-amyloid precursor protein.** *J Biol Chem* 2005, **280**:15464-70.
25. Huang Y, Liu XQ, Wyss-Coray T, Brecht WJ, Sanan DA, Mahley RW: **Apolipoprotein E fragments present in Alzheimer's disease brains induce neurofibrillary tangle-like intracellular inclusions in neurons.** *Proc Natl Acad Sci USA* 2001, **98**:8838-43.
26. Brecht WJ, Harris FM, Chang S, Tesseur I, Yu GQ, Xu Q, Dee Fish J, Wyss-Coray T, Buttini M, Mucke L, Mahley RW, Huang Y: **Neuron-specific apolipoprotein e4 proteolysis is associated with increased tau phosphorylation in brains of transgenic mice.** *J Neurosci* 2004, **24**:2527-34.
27. Harris FM, Brecht WJ, Xu Q, Tesseur I, Kekonius L, Wyss-Coray T, Fish JD, Masliah E, Hopkins PC, Scearce-Levie K, Weisgraber KH, Mucke L, Mahley RW, Huang Y: **Carboxyl-terminal-truncated apolipoprotein E4 causes Alzheimer's disease-like neurodegeneration and behavioral deficits in transgenic mice.** *Proc Natl Acad Sci USA* 2003, **100**:10966-71.
28. Fan D, Li Q, Korando L, Jerome WG, Wang J: **A monomeric human apolipoprotein E carboxyl-terminal domain.** *Biochemistry* 2004, **43**:5055-64.
29. Chang S, Ma Tr, Miranda RD, Balestra ME, Mahley RW, Huang Y: **Lipid- and receptor-binding regions of apolipoprotein E4**

fragments act in concert to cause mitochondrial dysfunction and neurotoxicity. *Proceedings of the National Academy of Sciences* 2005, **102**:18694-18699.
30. Mahley RW, Hui DY, Innerarity TL, Beisiegel U: **Chylomicron remnant metabolism. Role of hepatic lipoprotein receptors in mediating uptake.** *Arteriosclerosis* 1989, **9**:114-8.
31. Tanaka M, Vedhachalam C, Sakamoto T, Dhanasekaran P, Phillips MC, Lund-Katz S, Saito H: **Effect of carboxyl-terminal truncation on structure and lipid interaction of human apolipoprotein E4.** *Biochemistry* 2006, **45**:4240-7.
32. Pillot T, Goethals M, Najib J, Labeur C, Lins L, Chambaz J, Brasseur R, Vandekerckhove J, Rosseneu M: **Beta-amyloid peptide interacts specifically with the carboxy-terminal domain of human apolipoprotein E: relevance to Alzheimer's disease.** *J Neurochem* 1999, **72**:230-7.
33. Phu MJ, Hawbecker SK, Narayanaswami V: **Fluorescence resonance energy transfer analysis of apolipoprotein E C-terminal domain and amyloid beta peptide (1–42) interaction.** *J Neurosci Res* 2005, **80**:877-86.
34. Caspersen C, Wang N, Yao J, Sosunov A, Chen X, Lustbader JW, Xu HW, Stern D, McKhann G, Yan SD: **Mitochondrial Abeta: a potential focal point for neuronal metabolic dysfunction in Alzheimer's disease.** *Faseb J* 2005, **19**:2040-1.
35. Takahashi RH, Milner TA, Li F, Nam EE, Edgar MA, Yamaguchi H, Beal MF, Xu H, Greengard P, Gouras GK: **Intraneuronal Alzheimer abeta42 accumulates in multivesicular bodies and is associated with synaptic pathology.** *Am J Pathol* 2002, **161**:1869-79.
36. Martin BL, Schrader-Fischer G, Busciglio J, Duke M, Paganetti P, Yankner BA: **Intracellular Accumulation of beta-Amyloid in Cells Expressing the Swedish Mutant Amyloid Precursor Protein.** *J Biol Chem* 1995, **270**:26727-26730.
37. Chui DH, Tanahashi H, Ozawa K, Ikeda S, Checler F, Ueda O, Suzuki H, Araki W, Inoue H, Shirotani K, Takahashi K, Gallyas F, Tabira T: **Transgenic mice with Alzheimer presenilin 1 mutations show accelerated neurodegeneration without amyloid plaque formation.** *Nat Med* 1999, **5**:560-4.
38. Wilson CA, Doms RW, Lee VM: **Intracellular APP processing and A beta production in Alzheimer disease.** *J Neuropathol Exp Neurol* 1999, **58**:787-94.
39. Hartmann T: **Intracellular biology of Alzheimer's disease amyloid beta peptide.** *Eur Arch Psychiatry Clin Neurosci* 1999, **249**:291-8.
40. Lovestone S, Anderton BH, Hartley C, Jensen TG, Jorgensen AL: **The intracellular fate of apolipoprotein E is tau dependent and apoe allele-specific.** *Neuroreport* 1996, **7**:1005-8.
41. Hamilton RL, Wong JS, Guo LS, Krisans S, Havel RJ: **Apolipoprotein E localization in rat hepatocytes by immunogold labeling of cryothin sections.** *J Lipid Res* 1990, **31**:1589-603.
42. DeMattos RB, Thorngate FE, Williams DL: **A test of the cytosolic apolipoprotein E hypothesis fails to detect the escape of apolipoprotein E from the endocytic pathway into the cytosol and shows that direct expression of apolipoprotein E in the cytosol is cytotoxic.** *J Neurosci* 1999, **19**:2464-73.

The American Journal of Pathology, Vol. 175, No. 5, November 2009

DOI: 10.2353/ajpath.2009.090418

Neurobiology

Microglia Activated with the Toll-Like Receptor 9 Ligand CpG Attenuate Oligomeric Amyloid β Neurotoxicity in *in Vitro* and *in Vivo* Models of Alzheimer's Disease

Yukiko Doi,* Tetsuya Mizuno,* Yuki Maki,* Shijie Jin,* Hiroyuki Mizoguchi,† Masayoshi Ikeyama,‡ Minoru Doi,‡ Makoto Michikawa,§ Hideyuki Takeuchi,* and Akio Suzumura*

From the Department of Neuroimmunology and the Futuristic Environmental Simulation Center,† Research Institute of Environmental Medicine, Nagoya University, Nagoya; the Department of Materials Science and Engineering,‡ Nagoya Institute of Technology, Nagoya; and the Department of Alzheimer's Disease Research,§ National Institute for Longevity Sciences, National Center for Geriatrics and Gerontology, Aichi, Japan*

Soluble oligomeric amyloid β (oAβ) 1-42 causes synaptic dysfunction and neuronal injury in Alzheimer's disease (AD). Although accumulation of microglia around senile plaques is a hallmark of AD pathology, the role of microglia in oAβ1-42 neurotoxicity is not fully understood. Here, we showed that oAβ but not fibrillar Aβ was neurotoxic, and microglia activated with unmethylated DNA CpG motif (CpG), a ligand for Toll-like receptor 9, attenuated oAβ1-42 neurotoxicity in primary neuron-microglia co-cultures. CpG enhanced microglial clearance of oAβ1-42 and induced higher levels of the antioxidant enzyme heme oxygenase-1 in microglia without producing neurotoxic molecules such as nitric oxide and glutamate. Among subclasses of CpGs, class B and class C activated microglia to promote neuroprotection. Moreover, intracerebroventricular administration of CpG ameliorated both the cognitive impairments induced by oAβ1-42 and the impairment of associative learning in Tg2576 mouse model of AD. We propose that CpG may be an effective therapeutic strategy for limiting oAβ1-42 neurotoxicity in AD. ***(Am J Pathol 2009, 175:2121–2132; DOI: 10.2353/ajpath.2009.090418)***

The senile plaque is a pathological hallmark of Alzheimer's disease (AD). Fibrillar amyloid β (fAβ), a major component of senile plaques, induces tau hyperphosphorylation and neuronal dystrophy.[1,2] Soluble oligomeric Aβ (oAβ) has been reported to exhibit higher neurotoxicity than fAβ. Naturally secreted oAβ inhibits hippocampal long-term potentiation and disrupts synaptic plasticity in rats *in vivo*[3]. In addition, oAβ induces neuronal reactive oxygen species (ROS) through a mechanism requiring *N*-methyl-D-aspartate receptor activation.[4] Exposure to oAβ induces rapid and massive neuronal death, while fAβ is required at higher concentrations and for longer incubations to cause neuronal dystrophy.[5]

Microglia, macrophage-like cells in the central nervous system, cluster both in and around senile plaques and have been proposed to have pivotal roles in the pathogenesis of AD. Microglia activated with Aβ may be involved in the inflammatory component of AD.[6] Both fAβ and oAβ stimulate microglial secretion of proinflammatory cytokines, chemokines, complement components, and free radicals.[7] However, microglia also perform neu-

Supported in part by a grant-in-aid for scientific research (grant C), Global Centers of Excellence program "Integrated Functional Molecular Medicine for Neuronal and Neoplastic Disorders" funded by Ministry of Education, Culture, Sports, Science, and Technology of Japan, the Program for Promotion of Fundamental Studies in Health Sciences of the National Institute of Biomedical Innovation, the Hori Information Science Promotion Foundation, a grant-in-aid for Scientific Research on Priority Areas-Research on Pathomechanisms of Brain Disorders-from the Ministry of Education, Culture, Sports, Science, and Technology of Japan, and a grant from the Ministry of Health, Labor and Welfare of Japan (Comprehensive Research on Aging and Health grant H20-007).

Y.D. and T.M. contributed equally to this paper.

Accepted for publication July 30, 2009.

Supplemental material for this article can be found on *http://ajp.amjpathol.org*.

Address reprint requests to Tetsuya Mizuno, Department of Neuroimmunology, Research Institute of Environmental Medicine, Nagoya University, Furo-cho, Chikusa-ku, Nagoya 464-8601, Japan. E-mail: tmizuno@riem.nagoya-u.ac.jp.

roprotective functions such as releasing neurotrophic factors[8] and phagocytosing and degrading Aβ.[9,10]

Toll-like receptor (TLR) ligands enhance microglial phagocytosis of Aβ. Peptidoglycan, a TLR2 ligand, and unmethylated DNA CpG motifs (CpG), a TLR9 ligand, increase Aβ phagocytosis through the G protein-coupled formyl peptide receptor-like 2.[11,12] Similarly, the TLR4 ligand lipopolysaccharide increases phagocytosis through the CD14 receptor.[13] However, microglia activated with TLR ligands also produce neurotoxic molecules such as proinflammatory cytokines, nitric oxide (NO), ROS, and peroxynitrite.[14] In particular, lipopolysaccharide-activated microglia produce a large amount of glutamate, a neurotransmitter but also potent neurotoxin.[15] Thus, factors that increase microglial clearance of oAβ without producing inflammatory mediators are candidates for the treatment of AD.

Here, we investigated the role of microglia in neurotoxicity mediated by oAβ1-42. We found that microglia activated with a low dose of CpG attenuated the neurotoxic effects of oAβ1-42 without producing other neurotoxic molecules *in vitro*. Moreover, intracerebroventricular (ICV) administration of CpG ameliorated the cognitive impairment induced by ICV injection of oAβ1-42 and the impairment of associative learning in Tg2576 mouse model of AD.

Materials and Methods

Cell Culture

The protocols for animal experiments were approved by the Animal Experiment Committee of Nagoya University. Primary neuronal cultures were prepared from the cortices of embryonic day 17 (E17) C57BL/6 mice embryos as described previously.[8] Briefly, cortical fragments were dissociated into single cells in dissociation solution (Sumitomo Bakelite, Akita, Japan) and resuspended in Nerve Culture Medium (Sumitomo Bakelite). Neurons were plated onto 12-mm-polyethyleneimine-coated glass coverslips (Asahi Techno Glass, Chiba, Japan) at a density of 5×10^4 cells/well in 24-well multidishes and incubated at 37°C in a humidified atmosphere containing 5% CO_2. The purity of the cultures was >95% as determined by NeuN-specific immunostaining. Microglia were isolated on 14 days *in vitro* with the "shaking off" method previously described from primary mixed glial cell cultures prepared from newborn C57BL/6 mice.[16] Cultures were 97 to 100% pure as determined by Fc receptor-specific immunostaining and were maintained in Dulbecco's modified Eagle medium supplemented with 10% fetal calf serum, 5 μg/ml bovine insulin, and 0.2% glucose. Microglia were plated at a density of 7×10^4 cells/well in 8-well glass slides or at a density of 7×10^4 cells/well in 48-well multidishes. Neuron-microglia co-cultures were prepared as follows: 1×10^5 microglia in 100 μl of neuronal medium were added to neuronal cultures (5×10^4 neuronal cells) on 13 day *in vitro* in 24-well multidishes.

Preparations of Aβ Solutions

fAβ1-42 was prepared as described previously.[17] Briefly, synthetic human Aβ1-42 (Peptide Institute, Osaka, Japan) was dissolved in 0.02% ammonia solution at a concentration of 250 μmol/L, diluted to 25 μmol/L in PBS, and incubated at 37°C for 24 hours. oAβ1-42 was prepared as described previously.[18] Briefly, Aβ1-42 was dissolved to 1 mmol/L in 100% 1,1,1,3,3,3-hexafluoro-2-propanol. 1,1,1,3,3,3-Hexafluoro-2-propanol was dried by the vacuum desiccator and resuspended to 5 mmol/L in DMSO. To form oligomers, amyloid peptide was diluted to a final concentration of 100 μmol/L with Ham's F-12 and incubated at 4°C for 24 hours and then immediately added to cultures at a final concentration 5 μmol/L.

Transmission Electron Microscopy

To assess quaternary structures of Aβ, oAβ1-42 and fAβ1-42 solutions were spread on carbon-coated grids. Negative staining was performed with 3% phosphotungstic acid (pH 7.0). Proteins were then examined with a JEM-2000ExII Electron Microscope with an acceleration voltage of 160 kV.

Thioflavin T Assay

Optimum fluorescence measurements of amyloid fibrils were obtained at excitation and emission wavelength of 446 and 490 nm, respectively, with a reaction mixture containing 5 μmol/L thioflavin T (Nakalai tesque, Kyoto, Japan) and 50 mmol/L glycine-NaOH buffer (pH 8.5). Ten microliters of oAβ1-42 or fAβ1-42 solution was mixed with 100 μl of the reaction mixture, respectively.

Measurement of Heme Oxygenase-1, Interleukin-10, Matrix Metalloproteinase-9, Tumor Necrosis Factor-α, NO, and Glutamate

To measure factors produced by microglia treated with CpG and oAβ1-42, microglia were plated at a density of 7×10^4 cells/well (300 μl) in 48-well multidishes and then treated with 100 nmol/L CpG-DNA (HyCult Biotechnology, Uden, Netherlands), 100 nmol/L class A CpG (synthetic oligodeoxynucleotides (ODNs) 1585), class B CpG (ODN 1668), and class C CpG (ODN 2395). These CpG subtypes were from Alexis Biochemicals (San Diego, CA). After 3 hours of treatment with CpG, 5 μmol/L oAβ1-42 was added for 24 hours. Supernatants from microglia were assessed by ELISA kits for tumor necrosis factor-α (TNF-α) and interleukin (IL)-10 (BD Pharmingen, Franklin Lakes, NJ) and matrix metalloproteinase (MMP)-9 (R&D Systems, Minneapolis, MN). Cell extracts from microglia in extraction buffer (1% Nonidet P-40 in PBS) were measured for heme oxygenase-1 (HO-1) with an ELISA kit (Takara Bio, Mie, Japan). Measurement of NO was determined using the Griess reaction.[19] To measure glutamate, Glutamate Assay Kit colorimetric assay (Yamasa, Tokyo, Japan) was used as described previously.[20]

The mRNA expression of HO-1 was assessed by RT-PCR. Briefly, total RNA was extracted using the guanidinium thiocyanate method (RNeasy Mini Kit; Qiagen, Valencia, CA). cDNAs were generated by RT-PCR using SuperScript II (Invitrogen, Carlsbad, CA) and Ampli TaqDNA polymerase (Applied Biosystems, Branchburg, NJ) in the presence of the specific primers. HO-1 sense, 5′-CTATGTAAAGCGTCTCCA-3′; and HO-1 antisense, 5′-GTCTTTGTGTTCCTCTGTC-3′.

Measurement of ROS

To measure ROS in neuron-microglia co-cultures, we used the acetate ester form of 2′,7′-dichlorofluorescein diacetate (H_2DCFDA-AM) probe (Invitrogen). After neuron-microglia co-cultures were treated with or without 100 nmol/L CpG for 3 hours, cells were loaded with dye by replacing media with fresh nerve culture medium containing 5 μmol/L H_2DCFDA-AM for 30 minutes. After washing, culture medium containing 5 μmol/L oAβ1-42 was added and the fluorescence of the wells was measured. Fluorescent measurements were made using a Wallac 1420 ARVOMX (PerkinElmer Japan, Yokohama, Japan).

Immunocytochemistry

Neuronal, microglial, and neuron-microglia co-cultures were fixed with 4% paraformaldehyde for 30 minutes at room temperature, then blocked with 5% normal goat serum in PBS and permeabilized with 0.3% Triton X-100. Neurons were stained with rabbit polyclonal anti-microtubule-associated protein (MAP)-2 antibody (1/500; Chemicon, Temecula, CA) and secondary antibodies conjugated to Alexa 488 (1/1000; Invitrogen). Synthetic Aβ was stained with a mouse monoclonal anti-Aβ antibody (4G8) (1/1000; Chemicon) and secondary antibodies conjugated to Alexa 568 or 647. Microglia were stained with phycoerythrin-conjugated rat anti-mouse CD11b monoclonal antibody (1/300; BD Pharmingen) before fixation. Images were analyzed with a deconvolution fluorescent microscope system (BZ-8000; Keyence, Osaka, Japan). To assess neuronal death induced by Aβ, purified neurons (5×10^4 cells/well) were plated in 24-well multidishes. A total of 5 μM oAβ1-42 or fAβ1-42 was added to the cultures on 13 days *in vitro* for 24 hours. To assess neuronal death in neuron-microglia co-cultures, 3 hours after treatment with or without TLR ligands, 5 μmol/L oAβ1-42 was added to cultures for 24 hours. Surviving neurons were identified by cytoskeletal morphology of neurons as described previously.[8] Viable neurons stained strongly with an anti-MAP-2 antibody, whereas damaged neurons stained more weakly. The number of MAP-2-positive neurons was counted in representative areas per well. More than 200 neurons were examined in each of five independent trials by a scorer blind to the experimental condition. The number of untreated viable neurons was normalized to 100%.

Western Blotting

Neuronal cultures were treated with 5 μmol/L oAβ1-42 for 24 hours. Neuron-microglia co-cultures were pretreated with CpG for 3 hours before addition of 5 μmol/L oAβ1-42 for 24 hours. The supernatants of these cultures were collected. oAβ in 10-month-old-Tg 2576 mouse brain was extracted from the soluble, extracellular-enriched fraction as described previously.[21] Hemi-forebrains were harvested in 500 μl of solution containing 50 mmol/L Tris-HCl (pH 7.6), 0.01% Nonidet P-40, 150 mmol/L NaCl, 2 mmol/L EDTA, 0.1% SDS, and protease inhibitor mixture (Sigma-Aldrich, St. Louis, MO). Soluble, extracellular-enriched proteins were collected from mechanically homogenized lysates following centrifugation for 5 minutes at 3000 rpm.

Collected samples were mixed with sample buffer (200 mmol/L Tris-HCl, 8% SDS, and 1% glycerol). Proteins were separated on a 5 to 20% Tris-glycine SDS-polyacrylamide gel and transferred to Hybond-P polyvinylidene difluoride membrane (GE Healthcare UK, Buckinghamshire, UK). Membranes were blocked with 1% skim milk in Tris-buffered saline (TBS) containing 0.05% Tween20 (TBS-T). Blots were incubated in mouse anti-Aβ monoclonal antibody (6E10) (1/1000; Chemicon) diluted in 1% skim milk overnight at 4°C. Subsequently, membranes were washed in TBS-T 3 × 5 minutes and incubated with a horseradish peroxidase-conjugated anti-mouse IgG (1/5000; GE Healthcare) diluted in 1% skim milk for 1 hour. After washing in TBS-T for 1 × 15 minutes, 2 × 5 minutes, and TBS for 1 × 5 minutes, signals were visualized with SuperSignal West Pico Chemiluminescent Substrate (Thermo Fisher Scientific, Rockford, IL). The intensity of the bands was calculated by using CS Analyzer 1.0 (Atto, Tokyo, Japan).

Novel-Object Recognition Test in oAβ1-42-Induced Cognitive Impairment Mouse Model

oAβ (300 pmol/3 μl), CpG (100 nmol/L), or both oAβ and CpG were ICV injected as described previously.[22,23] The vehicle (PBS) was injected as the control. Briefly, a microsyringe with a 28-gauge stainless-steel needle 3.0 mm long was used for these experiments. C57/BL6 mice were anesthetized lightly with ether, and the needle was inserted unilaterally 1 mm to the right of the midline point equidistant from each eye, at an equal distance between the eyes and the ears and perpendicular to the plane of the skull. A single injection of 3 μl of peptide or vehicle was delivered gradually over 3 minutes. The injection site was confirmed in preliminary experiments. Neither insertion of the needle nor the volume of injection had a significant influence on survival and behavioral responses or cognitive functions.

The novel-object recognition test (NORT) was performed 7 to 8 days after ICV injection of oAβ1-42 or CpG as described previously.[24,25] The experimental apparatus consisted of a plexiglas open-field box (30 × 30 × 35 high cm), with a sawdust-covered floor. The apparatus

was located in a sound-attenuated room and was illuminated with a 60 lux light source. The NORT procedure consisted of three sessions: habituation, training, and retention. Each mouse was individually habituated to the box with 10 minutes of exploration in the absence of objects for 3 consecutive days (habituation session, days 4 to 6). During the training session, two novel objects were symmetrically fixed to the floor of the box, 8 cm from the walls, and each animal was allowed to explore in the box for 10 minutes (day 7). The objects were constructed from a golf ball, wooden column, and wooden triangular pyramid. They were different in shape and color but similar in size. An animal was considered to be exploring the object when its head was facing the object or it was touching or sniffing the object. The time spent exploring each object was recorded. After training, mice were immediately returned to their home cages. During the retention sessions (day 8), the animals were placed back into the same box 24 hours after the training session, but one of the familiar objects used during training had been replaced with a novel object. The animals were then allowed to explore freely for 5 minutes, and the time spent exploring each object was recorded. Throughout the experiments, the objects were used in a counterbalanced manner. A preference index in the retention session, a ratio of the amount of time spent exploring the novel object over the total time spent exploring both objects, was used to measure cognitive function. In the training session, the preference index was calculated as a ratio of the time spent exploring the object that was replaced by the novel object in the retention session over the total time exploring.

Cued and Contextual Fear-Conditioning Tests in Tg 2576 Mouse Model of AD

Cued and contextual fear conditioning tests were performed at 10 months of age according to previous report,[26] with minor modifications. For measuring basal levels of freezing response (preconditioning phase), mice were individually placed in a neutral cage (a block plexiglas box with abundant wood tips,30 × 30 × 40 high cm) for 1 minute, then in the conditioning cage (a transparent plexiglas box, 30 × 30 × 40 high cm) for 2 minutes. For training (conditioning phase), mice were placed in the conditioning cage, then a 15-second tone (80 dB) was delivered as a conditioned stimulus. During the last 5 seconds of the tone stimulus, a foot shock of 0.6 mA was delivered as an unconditioned stimulus through a shock generator (Neuroscience Idea). This procedure was repeated four times with 15-second intervals. Cued and contextual tests were performed 1 day after fear conditioning. For the contextual test, mice were placed in the conditioning cage, and the freezing response was measured for 2 minutes in the absence of the conditioned stimulus. For the cued test, the freezing response was measured in the neutral cage for 1 minute in the presence of a continuous-tone stimulus identical to the conditioned stimulus.

Stereotaxic injection was used for these experiments. Mice were anesthetized with sodium pentobarbital (50 mg/kg, i.p.) before stereotaxic implantation of a microinjection cannula into the right lateral ventricle (anteroposterior, −0.3 mm, and mediolateral, +1.0 mm, from the bregma, and dorsoventral, +2.5, from the skull according to the atlas of Franklin and Paxinos).[27] CpG was dissolved in PBS at a concentration of 10 or 100 nmol/L and was injected at a volume of 3 μl for 3 minutes. Same volume of PBS was injected to vehicle mouse. A week after injection, behavioral experiment was performed.

Immunohistochemistry

Immunohistochemistry was performed on brain tissue of mice after cued and contextual fear-conditioning test. Mice were transcardially perfused with ice-cold borate-buffered 4% paraformaldehyde under deep anesthesia. The brains were rapidly removed after decapitation. Brains were then postfixed overnight in periodate lysine paraformaldehyde, equilibrated in phosphate buffered 20% sucrose for 48 hours, and embedded into Tissue-Tek OCT compound (Sakura Finetechnical, Tokyo, Japan) and frozen at −80°C overnight. Coronal brain sections (20 μm) were cut with a cryostat. The sections were permeabilized with 1% Triton X-100 after blocking with 10% normal goat serum for 30 minutes. The cell nucleus was stained with Hoechst 33342 (1 μg/ml; Invitrogen). Aβ was stained with mouse monoclonal anti-Aβ antibody (4G8) (1/1000; Chemicon) and secondary antibodies conjugated to Alexa 488. Microglia were stained with a rat anti-mouse CD11b monoclonal antibody (1/1000; AbD Serotec, Oxford, UK) and secondary antibodies conjugated to Alexa 568. Images were collected and analyzed with a deconvolution fluorescent microscope system. Aβ load in immunostained tissue sections were quantified using BZ-analyzer (Keyence) as reported previously.[28] Seven sections were analyzed per animal. Total Aβ burden was quantified for the cortex and for the hippocampus on coronal plane sections stained with the monoclonal antibody 4G8. The cortical area was dorsomedial from the cingulate cortex and extended ventrolaterally to the rhinal fissure within the right hemisphere. Test areas (640 μm × 480 μm) were randomly selected. Total Aβ burden was calculated as the percentage of test area occupied by Aβ. Hippocampal measurements (600 × 600 μm) were performed similarly to the cortical analysis.

Statistical Analysis

Statistical significance of the biochemical experiments and the behavioral data were assessed with one-way analysis of variance, followed by post hoc Tukey test or Newman-Keuls test using GraphPad Prism version 5.0 (GraphPad Software, La Jolla, CA).

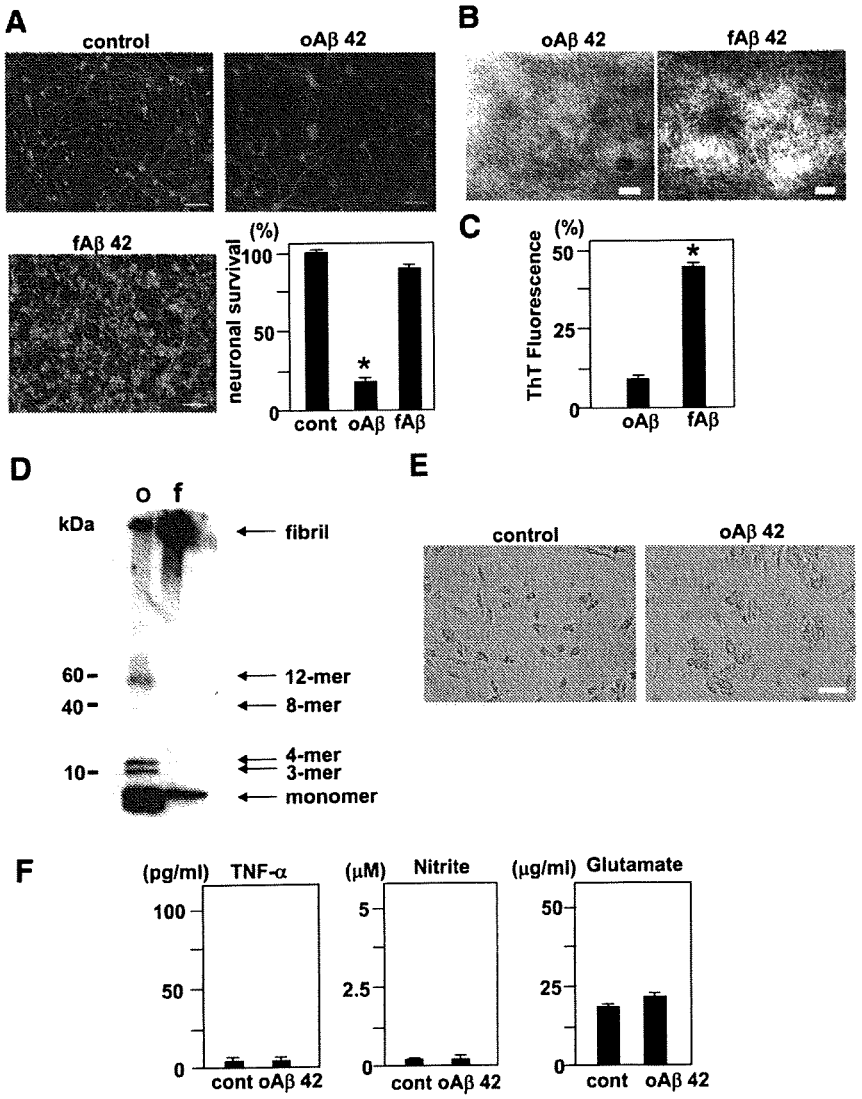

Figure 1. Neurotoxicity and morphologies of oAβ1-42 and fAβ1-42, and microglial response to oAβ1-42. **A:** The evaluation of neurotoxicity induced by oAβ1-42 and fAβ1-42. Neuronal cultures were treated with 5 μmol/L oAβ1-42 or fAβ1-42 for 24 hours. Neurons were stained with an anti-MAP-2 antibody (green). Aβ was stained with a mouse anti-amyloid β protein monoclonal antibody (4G8) (red). oAβ1-42 exhibited more striking neurotoxicity than fAβ1-42. Scale bar, 50 μm. Neuronal survival rate in oAβ1-42 treatment significantly decreased. $^*P < 0.05$ as compared with the rate in control cultures. Each column indicates the mean ± SEM ($n = 5$). **B:** Images of oAβ1-42 (**left**) and fAβ1-42 (**right**) collected with an electron microscope. Scale bar, 100 nm. **C:** Thioflavin T assay for oAβ1-42 and fAβ1-42. $^*P < 0.05$ as compared with the value of oAβ1-42. **D:** Western blot analysis of oAβ1-42 and fAβ1-42. oAβ1-42 (o) contained monomers, small oligomeric trimers (3-mer) and tetramers (4-mer), and the larger oligomers (octamers (8-mer) and dodecamers (12-mer)), whereas fAβ1-42 (f) contained monomers and fibrils. **E:** Microglial cultures were treated with or without 5 μmol/L oAβ1-42 for 24 hours. In a phase contrast, oAβ1-42 induced microglial adhesion. Scale bar, 50 μm. **F:** The measurement of TNF-α (**left**), nitrite (**middle**), and glutamate (**right**) produced by microglia activated with oAβ1-42. Microglial cultures were treated with 5 μmol/L oAβ1-42 for 24 hours. Each column indicates the mean ± SEM ($n = 7$).

Results

Neurotoxicity of oAβ1-42

First, we investigated the toxic effects of oAβ and fAβ on primary cortical neurons. Administration of 5 μmol/L oAβ1-42 to cortical cultures on DIV 13 for 24 hours resulted in significant neuronal death. The network of MAP-2-positive dendrites collapsed and neuronal survival decreased to 20% (Figure 1A). In contrast, administration of fAβ1-42 did not induce neuronal cell death, although Aβ deposition was observed on dendrites (Figure 1A). Thus, oAβ1-42 exhibits a more potent neurotoxicity than fAβ1-42. Both oAβ1-40 and fAβ1-40 did not induce neuronal cell death (Supplemental Figure S1, see *http://ajp.amjpathol.org*). We evaluated the morphology of oAβ1-42 and fAβ1-42 by transmission electron microscopy. We observed fine spherical particles of oAβ1-42 and fibril formation by fAβ1-42 (Figure 1B). The fluorescence of Thioflavin T, a marker for amyloid fibril formation, was associated with fAβ1-42 (Figure 1C). Western blotting with an antibody directed against Aβ (6E10) revealed that a solution of oAβ1-42 contained monomers, trimers (3-mer), tetramers (4-mer), and larger oligomers (octamers (8-mer) and dodecamers (12-mer)). In contrast, a solution of fAβ1-42 contained monomers and fibrils, but not oligomers (Figure 1D).

In primary microglial culture, administration of 5 μmol/L oAβ1-42 for 24 hours induced microglial adhesion (Figure 1E), but did not induce the production of neurotoxic mediators such as TNF-α, glutamate, or nitrite, a stable breakdown product of NO (Figure 1F).

Microglia Activated with CpG Attenuate the Neurotoxicity Induced by oAβ1-42

To define the role of microglia in the neurotoxicity of oAβ1-42, we evaluated neuronal survival in neuron-microglia co-cultures. Neurons stained with anti-MAP-2 antibody exhibited no detectable morphological abnormalities and possessed intact cell bodies and dendrites, and

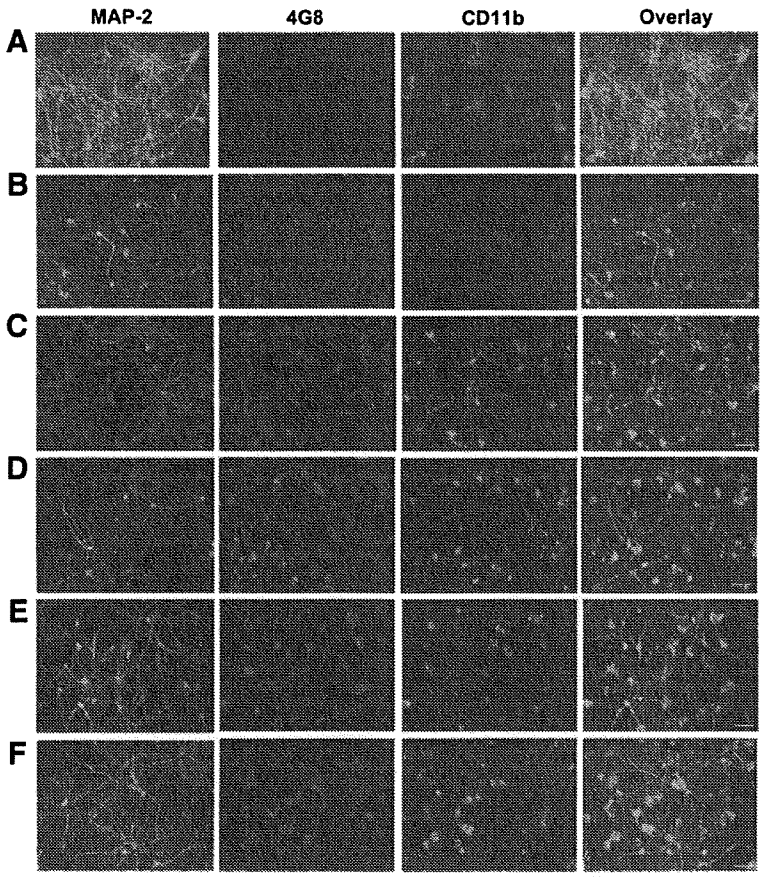

Figure 2. Protective effect of microglia activated with CpG against oAβ1-42 neurotoxicity. **A:** Representative deconvolution fluorescent images of control neuron-microglia co-cultures (1:2 of neuron: microglia). **B:** Neuronal cultures treated with 5 μmol/L oAβ1-42. **C:** Neuron-microglia co-cultures (1:2 neuron to microglia) treated with oAβ1-42. **D:** Neuron-microglia co-cultures stimulated with 1 nmol/L CpG and oAβ1-42 (**E**) or with 10 nmol/L CpG and oAβ1-42 (**F**) or with 100 nmol/L CpG and oAβ1-42. After 3 hours of treatment with CpG, cultures were treated with oAβ1-42 for 24 hours. Neurons were stained with an anti-MAP-2 antibody (green). Aβ was stained with 4G8 (red) and microglia were stained with a phycoerythrin-conjugated anti-CD11b antibody (blue). Scale bar, 50 μm. **G:** Neuronal survival rate was quantified as the percentage of intact neurons following treatment relative to control wells. The viability of untreated neurons (control) was normalized to 100%. $^{*}P < 0.05$ as compared with the survival rate of neuron-microglia co-cultures treated with oAβ1-42. Each column indicates the mean ± SEM ($n = 7$).

microglia stained with anti-CD11b antibody were also intact in unstimulated co-cultures (Figure 2A). After treatment of neuronal cultures with 5 μmol/L oAβ1-42 for 24 hours, the neuronal cells were severely damaged, and the survival rate decreased to 18% (Figure 2, B and G). Similarly, the neuronal survival rate was not improved in neuron-microglia co-cultures treated with oAβ1-42 (Figure 2, C and G), which implies that unstimulated microglia have not protective effect against oAβ1-42 neurotoxicity. Administration of CpG to neuronal cultures or neuron microglia co-cultures induced no toxic change (Supplemental Figure S2A, see *http://ajp.amjpathol.org*). After 3 hours of treatment with 1 nmol/L, 10 nmol/L, or 100 nmol/L CpG, 5 μmol/L oAβ1-42 was added to neuron-microglia co-cultures for 24 hours. The neuroprotective effect was not evident in culture with 1 nmol/L CpG (Figure 2, D and G). However, microglia treated with 10 or 100 nmol/L CpG prevented neuronal cell death, and the neuronal survival rate was significantly improved reaching 53 and 62%, respectively (Figure 2, E–G). In neuronal cultures, CpG did not attenuate the neurotoxicity induced by oAβ1-42 (Figure 2G). Moreover, 100 nmol/L CpG attenuated oAβ1-42-induced neurotoxicity for 48 hours, whereas other TLR ligands such as peptidoglycan and lipopolysaccharide did not (Supplemental Figure S2B, see *http://ajp.amjpathol.org*). We conclude from these findings that CpG-activated microglia have neuroprotective effect against oAβ1-42 neurotoxicity *in vitro*.

CpG-Activated Microglia Increase the Clearance of oAβ1-42, Produce the Antioxidant Enzyme HO-1 and Aβ-Degrading Enzyme MMP-9, and Release Fewer Neurotoxic Molecules

To elucidate the mechanisms of neuroprotection by microglia activated with CpG, we examined whether CpG increased the clearance of oAβ1-42. Western blot analysis revealed that there was no significant difference between the amount of oAβ1-42 present in the supernatants of neuronal cultures and in neuron-microglia co-cultures without CpG administration. (Figure 3A). However, CpG dose-dependently decreased the amount of oAβ1-42 in neuron-microglia co-cultures, especially treatment with 100 nmol/L CpG significantly decreased the amount of 3-, 4-, 8-, and 12-mer of oAβ1-42 (Figure 3, B and C). Moreover, we examined the effect of CpG on Aβ uptake by microglia alone at 1 and 24 hours time points. We found that CpG significantly enhanced microglial uptake of oAβ at both 1 and 24 hours (Supplemental Figure S3A, see *http://ajp.amjpathol.org*).

Because oxidative stress is a major component of oAβ1-42 neurotoxicity, we examined whether microglia activated with CpG express the antioxidant enzyme HO-1. CpG-activated microglia produced HO-1 in a dose-dependent manner. A total of 10 and 100 nmol/L CpG significantly increased the production of HO-1. The

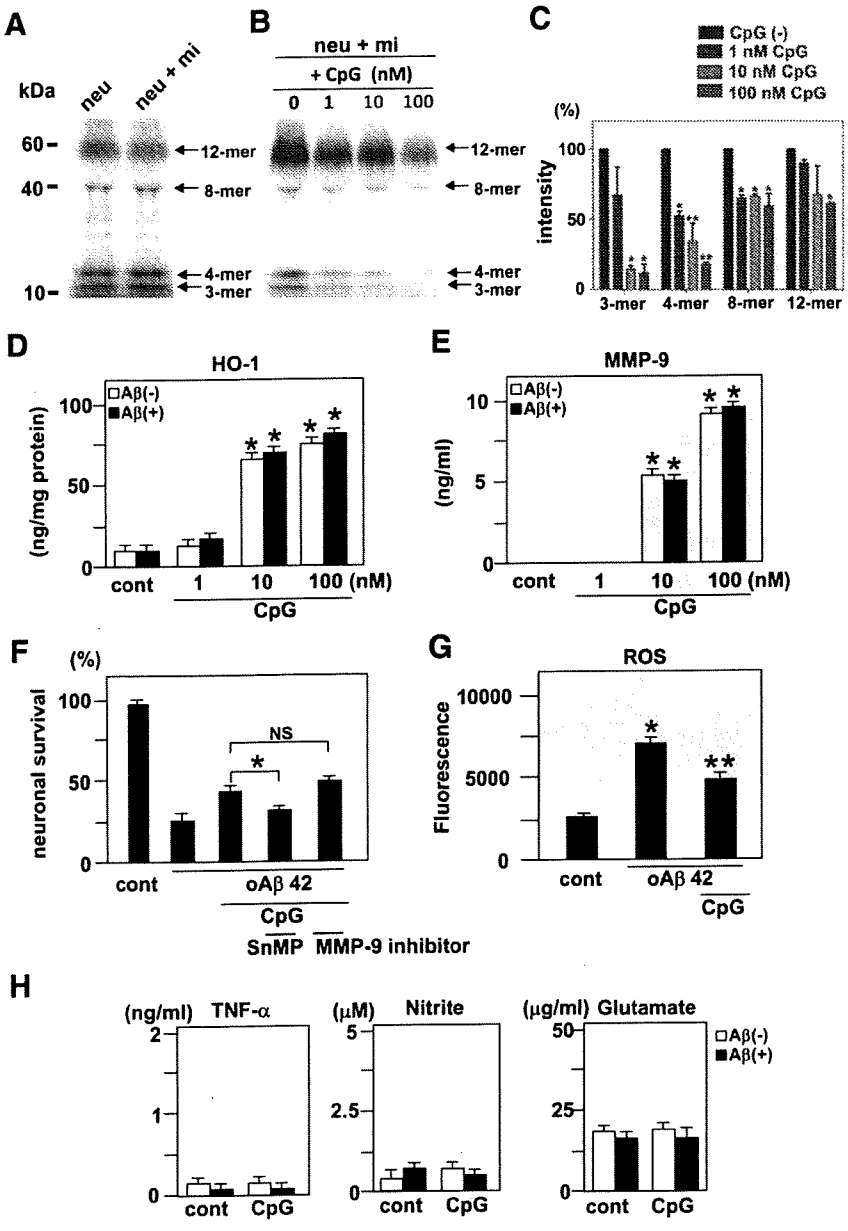

Figure 3. Clearance of oAβ1-42 and the production of HO-1, MMP-9, and neurotoxic molecules by microglia activated with CpG. **A:** Western blot analysis of oAβ1-42 in neuronal cultures (neu) and neuron-microglia co-cultures (neu + mi). Twenty-four hours after addition of 5 μmol/L oAβ1-42, oAβ1-42 present in the supernatants of these cultures was detected by Western blotting. **B:** Western blot analysis of oAβ1-42 in neuron-microglia co-cultures with CpG treatment. Neuron-microglia co-cultures (neu + mi) were treated with 5 μmol/L oAβ1-42 for 24 hours following 3 hours of treatment with 1, 10, or 100 nmol/L CpG. Microglia activated with CpG dose-dependently reduced the amount of oAβ1-42 in the supernatants. **C:** Semiquantification of oAβ1-42 in **B** by densitometric analysis. The amount of oAβ1-42 in neuron-microglial co-cultures without CpG (black) was normalized to 100%. oAβ1-42 in co-cultures treated with 1 nmol/L CpG (blue), 10 nmol/L CpG (green), or 100 nmol/L CpG (red) was calculated. $^{*}P < 0.05$ and $^{**}P < 0.01$ as compared with the intensity of oAβ1-42 in neuron-microglia co-cultures without CpG. Each column indicates the mean ± SEM ($n = 6$). The production of HO-1 (**D**) and MMP-9 (**E**) by microglia activated with CpG in the absence or presence of oAβ1-42. After 3 hours of treatment with CpG, microglial cultures were treated with or without oAβ1-42 for 24 hours. $^{*}P < 0.05$ as compared with untreated controls. Each column indicates the mean ± SEM ($n = 3$–5). **F:** The effect of HO-1 and MMP-9 on oAβ1-42 neurotoxicity. Neuron-microglia co-cultures were treated with 100 nmol/L CpG in the presence of 10 μmol/L tin-mesoporphyrin (SnMP) IX, a specific HO-1 inhibitor, or 50 nmol/L MMP-9 inhibitor for 3 hours, and then oAβ1-42 was added to the cultures for 24 hours. Tin-mesoporphyrin IX, but not the MMP-9 inhibitor, decreased neuronal survival rate. $^{*}P < 0.05$ as compared with CpG-treated cultures without inhibitors. Each column indicates the mean ± SEM ($n = 6$–9). **G:** The suppressive effect of CpG on ROS production by oAβ in the neuron microglia co-cultures. After neuron-microglia co-cultures were treated with or without 100 nmol/L CpG for 3 hours, cells were loaded with fresh nerve culture medium containing 5 μmol/L H_2DCFDA-AM for 30 minutes. After washing, culture medium containing 5 μmol/L oAβ1-42 was added and the increment of the fluorescence was calculated at 5 minutes. $^{*}P < 0.05$ as compared with untreated controls. $^{**}P < 0.05$ as compared with co-culture cells treated with oAβ1-42. Each column indicates the mean ± SEM ($n = 4$). **H:** The measurement of TNF-α (**left**), nitrite (**middle**), and glutamate (**right**) produced by microglia activated with 100 nmol/L CpG with or without oAβ1-42. After 3 hours treatment with CpG, microglial cultures were treated with or without oAβ1-42 for 24 hours. $^{*}P < 0.05$ as compared with untreated microglia. Each column indicates the mean ± SEM ($n = 7$).

production levels were not influenced by exposure to oAβ1-42 (Figure 3D). Since the anti-inflammatory cytokine IL-10 induces HO-1 expression by macrophages,[29] we also examined and confirmed that IL-10 induced HO-1 mRNA expression by microglia (Supplemental Figure S3B, see *http://ajp.amjpathol.org*). Although CpG induced IL-10 in microglia, the expression was suppressed by oAβ1-42 treatment (Supplemental Figure S3C, see *http://ajp.amjpathol.org*).

MMP-9 is also thought to play a neuroprotective role in AD because it degrades both oAβ and fAβ. A total of 10 and 100 nmol/L CpG significantly induced MMP-9 production in microglia with or without treatment of oAβ1-42 (Figure 3E). To determine whether HO-1 and MMP-9 contribute to the neuroprotective effects of CpG-activated microglia, we applied the specific HO-1 inhibitor tin-mesoporphyrin IX (Frontier Scientific, Logan, UT) and MMP-9 inhibitor (Merck, Darmstadt, Germany). The neuroprotective effect of CpG was abolished by treatment with 10 μmol/L tin-mesoporphyrin IX (Figure 3E). However, inhibition of MMP-9 with an MMP-9 inhibitor at 50 nmol/L did not influence the neuroprotective effect of CpG-activated microglia (Figure 3F). These results imply that HO-1 rather than MMP-9 may contribute to the